Proc Natl Acad Sci U S A. 2016 Feb 9;113(8):E1116–E1125. doi: 10.1073/pnas.1515741113

REDUCED CHLOROPLAST COVERAGE genes from *Arabidopsis thaliana* help to establish the size of the chloroplast compartment

Robert M Larkin [a,b,c,1], Giovanni Stefano [b], Michael E Ruckle [b,c,2], Andrea K Stavoe [b,3], Christopher A Sinkler [b,4], Federica Brandizzi [a,b], Carolyn M Malmstrom [a], Katherine W Osteryoung [a]

Author information Article notes Copyright and License information

PMCID: PMC4776492 PMID: 26862170

See "PNAS Plus Significance Statements" on page 1974.

Significance

Mechanisms that determine the cellular volume allocated to organelles are largely unknown. We demonstrate that in the plant *Arabidopsis thaliana*, a small gene family that encodes proteins of unknown function contributes to a mechanism that establishes the proportion of cellular volume devoted to chloroplasts. We show that this mechanism resides outside of the chloroplast by demonstrating that the protein that makes the greatest contribution to this mechanism resides in the cytoplasm and nucleus and that the trafficking of this protein between the cytoplasm and nucleus may regulate this mechanism. A deeper understanding of this mechanism may lead to the rational manipulation of chloroplast compartment size, which may lead to more efficient photosynthesis and increased yields from important crop plants.

Keywords: chloroplast coverage, chloroplast, plastid signaling, chlorophyll, *Arabidopsis*

Abstract

Eukaryotic cells require mechanisms to establish the proportion of cellular volume devoted to particular organelles. These mechanisms are poorly understood. From a screen for plastid-to-nucleus signaling mutants in *Arabidopsis thaliana*, we cloned a mutant allele of a gene that encodes a protein of unknown function that is homologous to two other *Arabidopsis* genes of unknown function and to *FRIENDLY*, which was previously shown to promote the normal distribution of mitochondria in *Arabidopsis*. In contrast to *FRIENDLY*, these three homologs of *FRIENDLY* are found only in photosynthetic organisms. Based on these data, we proposed that *FRIENDLY* expanded into a small gene family to help regulate the energy metabolism of cells that contain both mitochondria and chloroplasts. Indeed, we found that knocking out these genes caused a number of chloroplast phenotypes, including a reduction in the proportion of cellular volume devoted to chloroplasts to 50% of wild type. Thus, we refer to these genes as *REDUCED CHLOROPLAST COVERAGE* (*REC*). The size of the chloroplast compartment was reduced most in *rec1* mutants. The REC1 protein accumulated in the cytosol and the nucleus. REC1 was excluded from the nucleus when plants were treated with amitrole, which inhibits cell expansion and chloroplast function. We conclude that REC1 is an extraplastidic protein that helps to establish the size of the chloroplast compartment, and that signals derived from cell expansion or chloroplasts may regulate REC1.

Chloroplasts drive plant growth, development, and reproduction by converting solar energy into biologically useful forms of energy. Thus, the biogenesis and function of chloroplasts underpin crop yields and, indeed, life on Earth. Chloroplasts develop from proplastids during germination and leaf development (1). After chloroplast biogenesis, chloroplasts divide by binary fission. A number of mutant alleles enhance or reduce the size of individual chloroplasts by attenuating or promoting chloroplast division (2). Regardless of the size of individual chloroplasts, the proportion of cellular volume devoted to all chloroplasts appears indistinguishable from wild type in these mutants (3–5). Thus, the mechanism that establishes the size of the chloroplast compartment appears distinct from the mechanisms of chloroplast division.

The cell expansion that drives the expansion of leaves also drives the proliferation of chloroplasts. Indeed, the proliferation of chloroplasts is so tightly correlated with cell expansion that the ratio of the size of the chloroplast compartment to the size of mesophyll cells is constant, regardless of cell size (2, 6, 7). Cell type exerts a major influence over the proportion of cellular volume devoted to the chloroplast. For instance, the size of the chloroplast compartment in mesophyll cells is larger than in epidermal cells. Thus, an extraplastidic mechanism appears to determine the size of the chloroplast compartment (6). However, during the expansion of leaves, chloroplasts are not completely submissive to the cell. Indeed, chloroplast dysfunction inhibits the expansion of leaves (8).

Although mechanisms that establish the proportion of cellular volume devoted to particular organelles are of fundamental importance to biology, these mechanisms remain poorly understood (2). In the particular case of

chloroplasts, understanding these mechanisms may lead to significant advances for agriculture. For example, introducing C_4 photosynthesis into rice, a plant that performs C_3 photosynthesis, is one strategy for potentially increasing yields from this important crop (9). C_3 and C_4 leaves are distinct at the metabolic, cellular, and anatomical levels (9, 10). One of the conserved features of C_4 leaves is the increase and decrease in the size of the chloroplast compartment in bundle sheath and mesophyll cells, respectively, relative to C_3 leaves (10). The engineering of C_4 photosynthesis in important C_3 crops, such as rice, is thought to depend on the ability to rationally manipulate the size of the chloroplast compartment (11).

We performed a screen for plastid-to-nucleus signaling mutants in *Arabidopsis thaliana* (12). From this screen, we obtained one mutant allele of a gene that encodes a protein of unknown function. This gene is homologous to two *Arabidopsis* genes that encode proteins of unknown function and to *FRIENDLY*. *FRIENDLY* and its orthologs promote the normal distribution of mitochondria in *Arabidopsis* and in nonphotosynthetic organisms (13). However, these three *Arabidopsis* homologs of *FRIENDLY* are found only in photosynthetic organisms. Based on these data, we thought that *FRIENDLY* may have expanded into a small gene family to help manage the energy metabolism of cells that contain both chloroplasts and mitochondria. We tested this idea by examining the phenotypes of mutants in which one, two, three, or all four of these genes are knocked out. We found that these mutants exhibited a number of chloroplast phenotypes, including a smaller chloroplast compartment relative to wild type. Thus, we named these genes *REDUCED CHLOROPLAST COVERAGE* (*REC*). We also found that the protein that contributes most to establishing the size of the chloroplast compartment, REC1, localizes to both the nucleus and the cytosol, and we provide evidence that signals derived from dysfunctional chloroplasts or the inhibition of cell expansion may regulate the nucleocytoplasmic partitioning of REC1.

Results

Cloning and Characterizing *rec1-1*.

We obtained one mutant allele of *REC1* that we named *rec1-1* from a screen for *genomes uncoupled* (*gun*) mutants (12). *gun* alleles disrupt the plastid-to-nucleus signaling that down-regulates photosynthesis-associated nuclear gene (PhANG) expression when chloroplast biogenesis is blocked. Thus, *gun* mutants express higher levels of PhANGs than wild type when chloroplast biogenesis is blocked (8). In addition to a *gun* phenotype, *rec1-1* greens after seedlings are grown in far-red light and then transferred to white light (Fig. 1*A* and *SI Appendix*, Fig. S1*A*). When wild-type seedlings are grown in far-red light, they overaccumulate the chlorophyll precursor protochlorophyllide. In white light, these elevated levels of protochlorophyllide block chloroplast biogenesis by inducing increases in the levels of singlet oxygen (14, 15). We mapped this greening phenotype to a 70-kb interval near the top of chromosome 1 (*SI Appendix*, Fig. S1*B*). We sequenced seven genes in this interval. We found a C-to-T transition that causes a nonsense mutation in the codon that encodes Q1415 of At1g01320 (*SI Appendix*, Fig. S1 *C* and *D*). At1g01320 encodes a protein of unknown function with a calculated mass of 200 kDa. This protein contains three tetratricopeptide repeats (TPRs) and 106 residues near

the carboxyl terminus that are 29% proline (*SI Appendix*, Fig. S1*D*). TPRs contribute to the protein–protein interactions that underpin diverse biological processes (16).

Fig. 1.

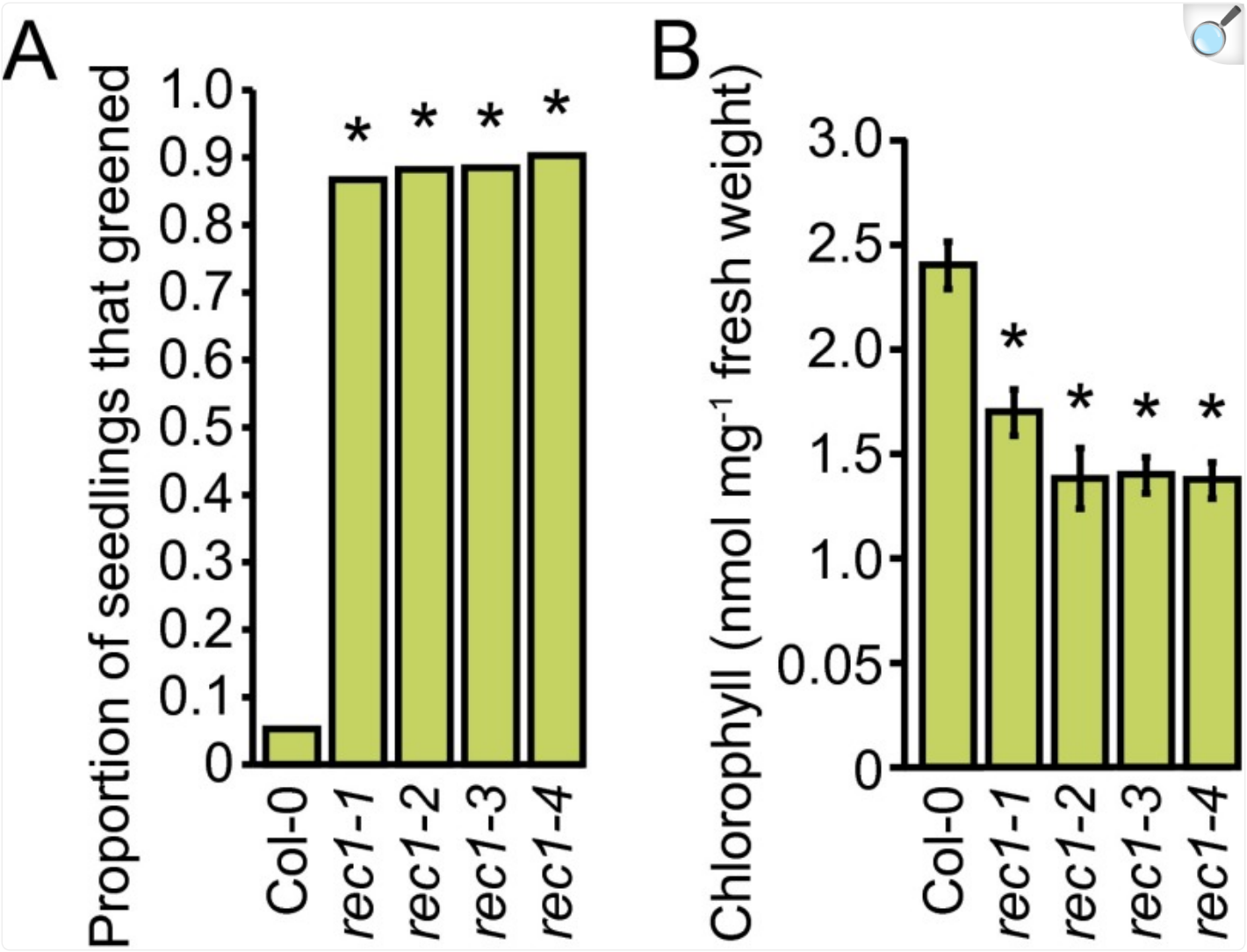

Open in a new tab

Chlorophyll phenotypes of *rec1* mutants. (*A*) The far-red block of greening phenotype of four *rec1* mutants. A far-red block of greening experiment was performed as described in *SI Appendix, Materials and Methods*. The proportions of seedlings that greened are indicated (n = 188–234; numbers were pooled from two biological replicates). The asterisk indicates a statistically significant difference relative to wild type (Col-0) ($P <$ 0.0001). (*B*) Chlorophyll phenotypes of *rec1* mutants. Plants were grown on soil for 24 d. Six biological replicates were analyzed for wild type (Col-0) and each mutant. Error bars indicate 95% confidence intervals. The asterisk indicates a statistically significant difference relative to wild type (Col-0) ($P < 0.0001$).

We obtained three publicly available T-DNA insertion mutants with insertions in At1g01320. We named these T-DNA insertion alleles *rec1-2*, *rec1-3*, and *rec1-4*. We found reduced levels of mRNA transcribed from At1g01320 in all of these mutants (*SI Appendix*, Fig. S2). We also analyzed these mutants by immunoblotting with affinity-purified antibodies raised against fragments of the protein encoded by At1g01320 that spanned from P1419 to F1673 (*SI Appendix*, Fig. S3*A*). When whole-leaf extracts were analyzed by immunoblotting, these antibodies recognized a single band in an extract that was prepared from wild type (*SI Appendix*, Fig. S3*B*). Based on the mobility of this protein in a 5% SDS gel (*SI Appendix*, Fig. S3*D*), we estimated that its mass is 240 kDa. This 240-kDa protein does not accumulate to detectable levels in *rec1-1*, *rec1-2*, *rec1-3*, or *rec1-4* (*SI Appendix*, Fig. S3 *B* and *C*).

We found that, similar to the *rec1-1* allele, the three T-DNA insertion alleles inhibited the far-red block of greening (Fig. 1*A*). We found that the chlorophyll levels in *rec1-1* were 71% of wild type. In contrast, we found that the chlorophyll levels of *rec1-2*, *rec1-3*, and *rec1-4* were 57–58% of wild type (Fig. 1*B*) and 81–82% of *rec1-1* ($P = 0.001$–0.006). We conclude that *rec1-1* attenuated the accumulation of chlorophyll and that *rec1-2*, *rec1-3*, and *rec1-4* are null alleles. These data are consistent with *rec1-1* expressing a truncated protein that promotes the accumulation of chlorophyll. We were not able to detect such a truncated protein because our antibodies bind residues that are carboxyl-terminal to Q1415.

To test whether the three T-DNA insertion mutants are *gun* mutants, we grew them on media that contained either norflurazon or lincomycin. Norflurazon and lincomycin specifically block chloroplast biogenesis by distinct mechanisms and severely down-regulate the expression of PhANGs, such as the genes encoding the light harvesting chlorophyll *a*/*b*-binding proteins of photosystem II (*Lhcb*) and the small subunit of RuBisCO (*RbcS*) (8). We found that *rec1-1* accumulated 3.2- to 4.3-fold more *Lhcb1.2* than wild type and that *rec1-2*, *rec1-3*, and *rec1-4* accumulated significantly more *Lhcb1.2* mRNA than wild type (*SI Appendix*, Fig. S4). However, *rec1-2*, *rec1-3*, and *rec1-4* accumulated significantly less *Lhcb1.2* mRNA than *rec1-1* ($P < 0.0001$–0.009) (*SI Appendix*, Fig. S4). We observed a similar trend with *RbcS1A* expression (*SI Appendix*, Fig. S4). In contrast, *gun1-101* (12), a null allele of a relatively well studied *GUN* gene (8), induced 13- and 35-fold increases in *Lhcb1.2* expression when chloroplast biogenesis was blocked with norflurazon and lincomycin treatments, respectively (*SI Appendix*, Fig. S4). These data provide evidence that norflurazon treatments activate a repressive plastid-to-nucleus signaling mechanism that is not activated by lincomycin treatments or that an inductive mechanism present in lincomycin-treated seedlings is absent in norflurazon-treated seedlings.

In untreated seedlings, *Lhcb1.2* mRNA accumulated to significantly lower levels in *rec1-2*, *rec1-3*, and *rec1-4* than in wild type (*SI Appendix*, Fig. S4), which is consistent with the chlorophyll-deficient phenotypes of these mutants (Fig. 1*B*). The levels of *RbcS1A* mRNA were not significantly different in the untreated wild type and *rec1* mutants (*SI Appendix*, Fig. S4). Based on these data, we conclude that these *rec1* alleles specifically disrupted the plastid-regulated expression of these PhANGs and that At1g01320 is *REC1*.

Our characterization of these *rec1* alleles indicates that *rec1-1* behaves as a loss-of-function allele when the far-red block of greening and the chlorophyll accumulation phenotypes are scored and that *rec1-1* enhances the levels of PhANG expression relative to other mutant alleles of *REC1* when the *gun* phenotype is scored. A truncated REC1 protein that is partially active may underpin these phenotypes. There is precedence for mutant alleles causing both loss-of-function and gain-of-function phenotypes (17, 18).

Characterization of the *REC* Gene Family Mutants.

The REC1 protein is homologous to three other *Arabidopsis* proteins that are encoded by At4g28080, At1g15290, and *FRIENDLY* (At3g52140) (*SI Appendix*, Fig. S5). The proteins encoded by At4g28080 and At1g15290 have no known function. Loss-of-function alleles of *FRIENDLY* and its orthologs in *Dictyostelium discoideum*, *Saccharomyces cerevisiae*, and *Drosophila melanogaster* cause mitochondrial clustering (19). FRIENDLY and orthologous proteins were reported to perform a variety of functions, such as binding and regulating atypical protein kinase C (20), binding mRNAs that encode mitochondrial proteins and promoting the biogenesis of mitochondria (21), and promoting intermitochondrial associations before mitochondrial fusion (13). The calculated masses of the proteins that are encoded by At4g28080, At1g15290, and *FRIENDLY* are 200 kDa, 180 kDa, and 150 kDa, respectively. We named At4g28080 and At1g15290 *REC2* and *REC3*, respectively, based on their derived amino acid sequence similarity to REC1. REC1 is more similar to REC2 and REC3 than to FRIENDLY (*SI Appendix*, Fig. S5). Homologs of *REC1*, *REC2*, *REC3*, and *FRIENDLY* are present in other plant species (*SI Appendix*, Fig. S6). In contrast, eukaryotes that do not perform photosynthesis contain only orthologs of *FRIENDLY*, usually as a single-copy gene (*SI Appendix*, Fig. S6).

To test whether *REC2*, *REC3*, and *FRIENDLY* contribute to the same or different processes as *REC1*, we obtained T-DNA insertion alleles for each of these genes. We found that T-DNA insertions reduced the levels of mRNA transcribed from these genes (*SI Appendix*, Fig. S2). In *REC3* mutants, the low levels of mRNA are not expected to encode functional proteins because the insertions are in exons. In *REC2* and *FRIENDLY* mutants, the reduced levels of mRNA might express truncated proteins that are not functional. Indeed, three independent T-DNA insertions into *REC2* caused chlorophyll to accumulate at significantly lower levels than in wild type, and these reduced levels of chlorophyll were not significantly different from each other ($P = 0.3–0.6$) (*SI Appendix*, Fig. S7*A*). We conclude that these three alleles are nulls. Based on the robust mitochondrial clustering phenotype of the T-DNA insertion allele of *FRIENDLY* (*SI Appendix*, Fig. S7*B*), we conclude that this allele is either a null or a strong loss-of-function allele.

To determine the full impact of these four genes on chloroplast-related processes, we prepared double, triple, and quadruple mutants with *rec1-3*, *rec2*, *rec3-1*, and *friendly* in all possible combinations. We found that *rec2*, *rec3-1*, *rec3-2*, and *friendly* exhibited a far-red block of greening that was more similar to wild type than to *rec1-1* (*SI Appendix*, Fig. S8*A*). We found that after 3 d of growth in far-red light, protochlorophyllide accumulated to significantly lower levels in *rec1-3* than in wild type, protochlorophyllide accumulated to significantly higher levels in *friendly* than in wild type, and protochlorophyllide levels were not significantly different from wild type in *rec2* and *rec3-1* (*SI Appendix*,

Fig. S8*B*). Significantly less protochlorophyllide accumulated in double and triple mutants containing *rec1-3* and the quadruple mutants relative to the relevant single, double, and triple mutants ($P < 0.0001$–0.005). Significantly more protochlorophyllide accumulated in *rec3-1 friendly*, *rec1-3 rec3-1 friendly*, *rec1-3 rec2 friendly*, and *rec1-3 rec2 rec3-1 friendly* than in *rec3-1*, *rec1-3 rec3-1*, *rec1-3 rec2*, and *rec1-3 rec2 rec3-1*, respectively ($P = 0.0003$–0.02). We conclude that mutant alleles of *REC1* inhibit the far-red block of greening by reducing the levels of protochlorophyllide.

Attenuating phytochrome A signaling inhibits the far-red block of greening (15). Perhaps the simplest way to test for defects in phytochrome A signaling is to measure hypocotyl lengths in far-red light. We found that, in the dark, the lengths of the *rec1-3* hypocotyls were not significantly different from wild type but that those of *rec1-3 rec2 rec3-1 friendly* were 11% shorter (*SI Appendix*, Fig. S8*C*). However, we found that in 3 $\mu mol \cdot m^{-2} \cdot s^{-1}$ far-red light, the hypocotyls of *rec1-3* and *rec1-3 rec2 rec3-1 friendly* were not significantly different from wild type ($P = 0.4$–0.5) (*SI Appendix*, Fig. S8*D*). We conclude that the inhibition of the far-red block of greening in *rec1* mutants is probably not caused by defects in phytochrome A signaling.

We found that when chloroplast biogenesis was blocked with a lincomycin treatment, *Lhcb1.2* expression in *rec2* and *rec3-1* was 69% and 68% of the levels observed in wild type, respectively. In *friendly*, *RbcS1A* expression was increased 1.5-fold but *Lhcb1.2* expression was not significantly different from wild type (*SI Appendix*, Fig. S8*E*). Double and triple mutants containing *rec1-3* and *friendly* tended to exhibit *gun* phenotypes, as did the quadruple mutant, whereas the double and triple mutants containing *rec2* and *rec3-1* generally did not exhibit *gun* phenotypes (*SI Appendix*, Fig. S8*E*). The most robust *gun* phenotype was observed for *rec1-3 rec2 friendly*, which accumulated 3.3- and 2.2-fold more mRNA from *Lhcb1.2* and *RbcS1A*, respectively, than wild type (*SI Appendix*, Fig. S8*E*). Thus, this gene family makes significant but minor contributions to the plastid regulation of these PhANGs relative to *GUN1* (*SI Appendix*, Fig. S4).

REC gene family mutants appear chlorophyll-deficient (*SI Appendix*, Fig. S9). These chlorophyll deficiencies ranged from uniform chlorophyll deficiencies to virescence in *rec1-3 rec3-1* and *rec1-3 rec3-1 friendly* (*SI Appendix*, Fig. S9). We quantified the chlorophyll levels of these mutants and found that *rec1-3* and *rec2* accumulated 63% and 81% of the chlorophyll found in wild type, respectively (Fig. 2). In several instances, combinations of these alleles enhanced the chlorophyll-deficient phenotypes of *rec1-3* and *rec2*. The most extreme examples were *rec1-3 rec2*, *rec1-3 rec2 rec3-1*, and *rec1-3 rec2 rec3-1 friendly*, which accumulated 31%, 21%, and 16% of the chlorophyll found in wild type, respectively (Fig. 2). In contrast to *rec1-3* and *rec2*, there was no significant difference in the levels of chlorophyll that accumulated in *rec3-1*, *friendly*, *rec3-1 friendly*, and wild type ($P = 0.2$–0.8) (Fig. 2). Additionally, *rec3-1* and *friendly* did not affect the accumulation of chlorophyll in *rec1-3 friendly*, *rec2 friendly*, and *rec2 rec3-1* ($P = 0.1$–0.9) (Fig. 2). However, *rec1-3 rec3-1* and *rec1-3 rec2 rec3-1* accumulated significantly less chlorophyll than *rec1-3* and *rec1-3 rec2* ($P < 0.0001$), respectively (Fig. 2). Thus, *rec3-1* attenuated the accumulation of chlorophyll in particular genetic contexts. Additionally, *rec1-3 rec2 friendly* accumulated significantly more chlorophyll than *rec1-3 rec2* ($P = 0.0004$) and *rec1-3 rec2 rec3-1 friendly* accumulated significantly less chlorophyll than *rec1-3 rec2 rec3-1* ($P = 0.002$) (Fig. 2). Thus, the effect of *friendly* on the accumulation of chlorophyll depended on the genetic context.

Fig. 2.

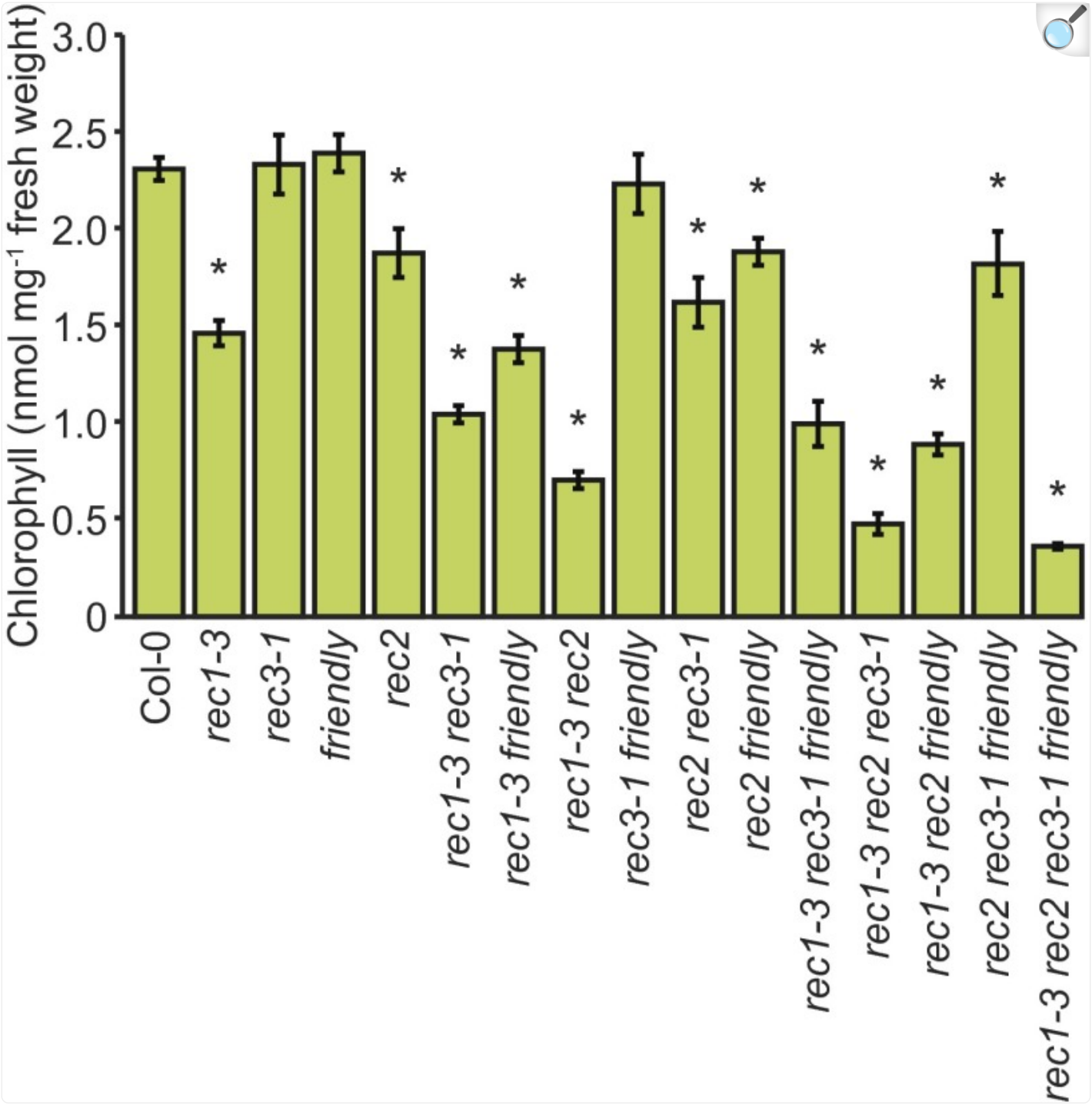

Open in a new tab

Chlorophyll levels in the *REC* gene family mutants. Plants were grown on soil for 24 d. Six biological replicates were analyzed for wild type (Col-0) and each mutant. Error bars indicate 95% confidence intervals. The asterisk indicates a statistically significant difference relative to wild type ($P < 0.0001–0.0003$).

The chloroplast ultrastructure in many of the mutants resembled wild type (*SI Appendix*, Fig. S10). The chloroplast ultrastructures of chlorophyll-deficient mutants typically resemble wild type (22, 23). The most severely chlorophyll-deficient mutants (Fig. 2) tended to have long and thin chloroplasts relative to wild type (*SI Appendix*, Fig. S11). Similar phenotypes were not reported for tetrapyrrole biosynthesis mutants, such as the severely chlorophyll-deficient *gun4 hy1* and *gun5 hy1* double mutants (22). Holes were observed in the chloroplasts of *rec1-3 rec2 rec3-1* that were surrounded by double membranes (*SI Appendix*, Fig. S12). These holes probably resulted from the sectioning of cytosolic protrusions into the chloroplasts that do not disrupt the chloroplast double membrane. Consistent with this interpretation, a mitochondrion was found in one of these holes (*SI Appendix*, Fig. S12).

The grana thylakoids of the mutants appeared similar to wild type, but *rec1 rec2 rec3-1* contained fewer grana thylakoids than wild type (*SI Appendix*, Fig. S13). A reduction in the number of grana thylakoids is not commonly observed in *Arabidopsis* mutants unless the chlorophyll deficiencies are severe (22–24). The thylakoid membranes appeared swollen in four *friendly* mutants (*SI Appendix*, Fig. S14) and similar to wild type in the other *friendly* mutants (*SI Appendix*, Fig. S13). Swelling of the thylakoid membranes was not reported previously for *friendly* mutants (13, 25). These data are consistent with complex interactions among these alleles affecting the ability of the thylakoid membranes to withstand osmotic pressure (26).

To further characterize the chloroplast defects of these mutants, we imaged the chloroplasts in live cells from the abaxial epidermal cells to the cortical region of the spongy mesophyll cells in leaves using confocal laser scanning microscopy. We found a number of differences relative to wild type. These differences included a tendency of the chloroplasts to localize along the anticlinal walls of mesophyll cells, enhanced chlorophyll fluorescence in both the mesophyll and epidermal cells, and fewer chloroplasts in the mesophyll cells in particular triple mutants and the quadruple mutant (Fig. 3*A* and *SI Appendix*, Fig. S15). The chloroplasts of the mesophyll cells residing along the anticlinal walls and the increases in chlorophyll fluorescence are consistent with increased sensitivity to light (27, 28). To test whether a potentially enhanced sensitivity to light led to a rise in the levels of reactive oxygen species, we stained leaves with 3,3′-diaminobenzidine (DAB) and nitrotetrazolium blue (NBT) to detect hydrogen peroxide and superoxide, respectively. These mutants appear to accumulate variable levels of reactive oxygen species (*SI Appendix*, Fig. S16).

Fig. 3.

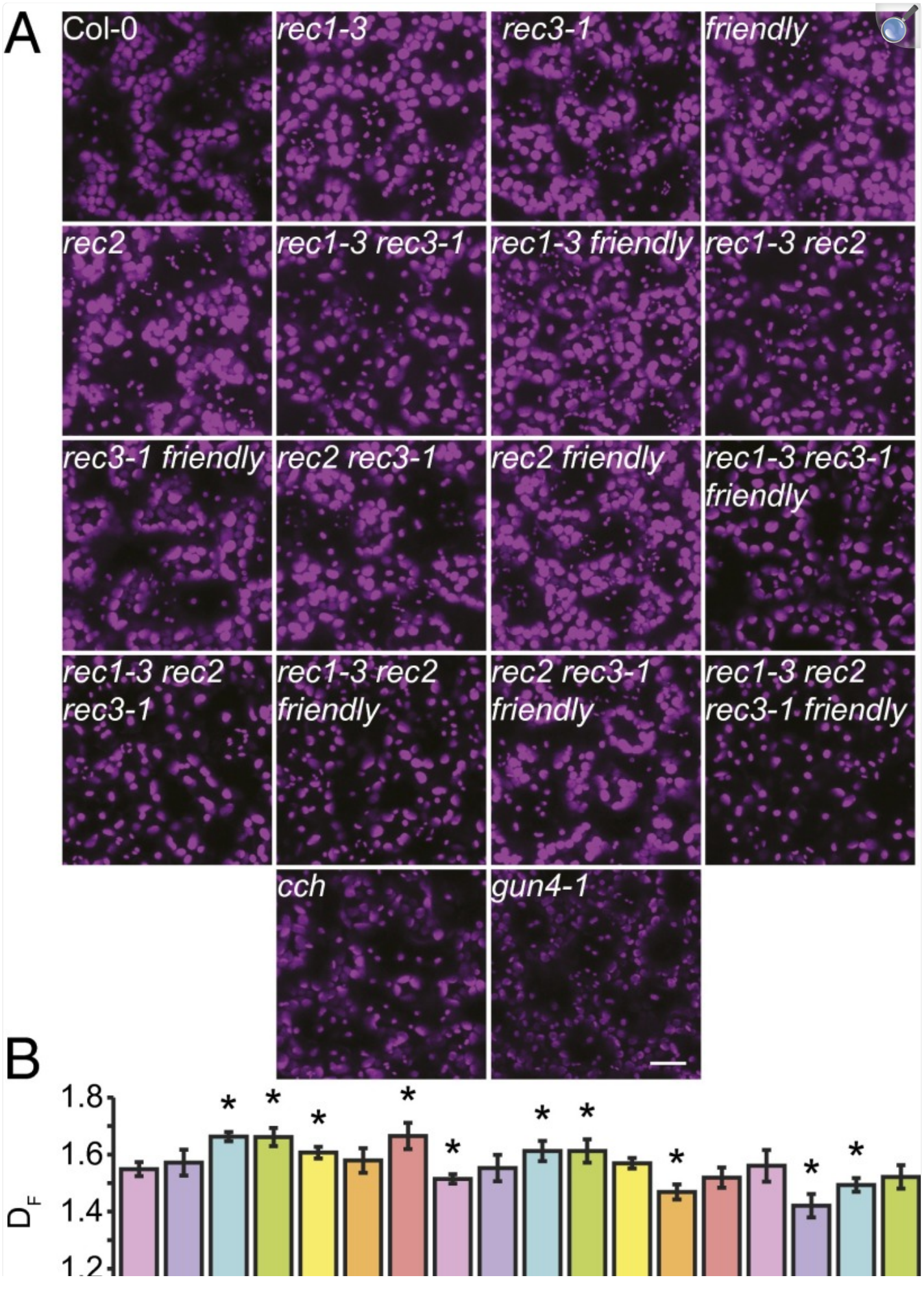
A
Col-0
rec1-3
rec3-1
friendly
rec2
rec1-3 rec3-1
rec1-3 friendly
rec1-3 rec2
rec3-1 friendly
rec2 rec3-1
rec2 friendly
rec1-3 rec3-1 friendly
rec1-3 rec2 rec3-1
rec1-3 rec2 friendly
rec2 rec3-1 friendly
rec1-3 rec2 rec3-1 friendly
cch
gun4-1
B
1.8
1.6
1.4
1.2
D_F

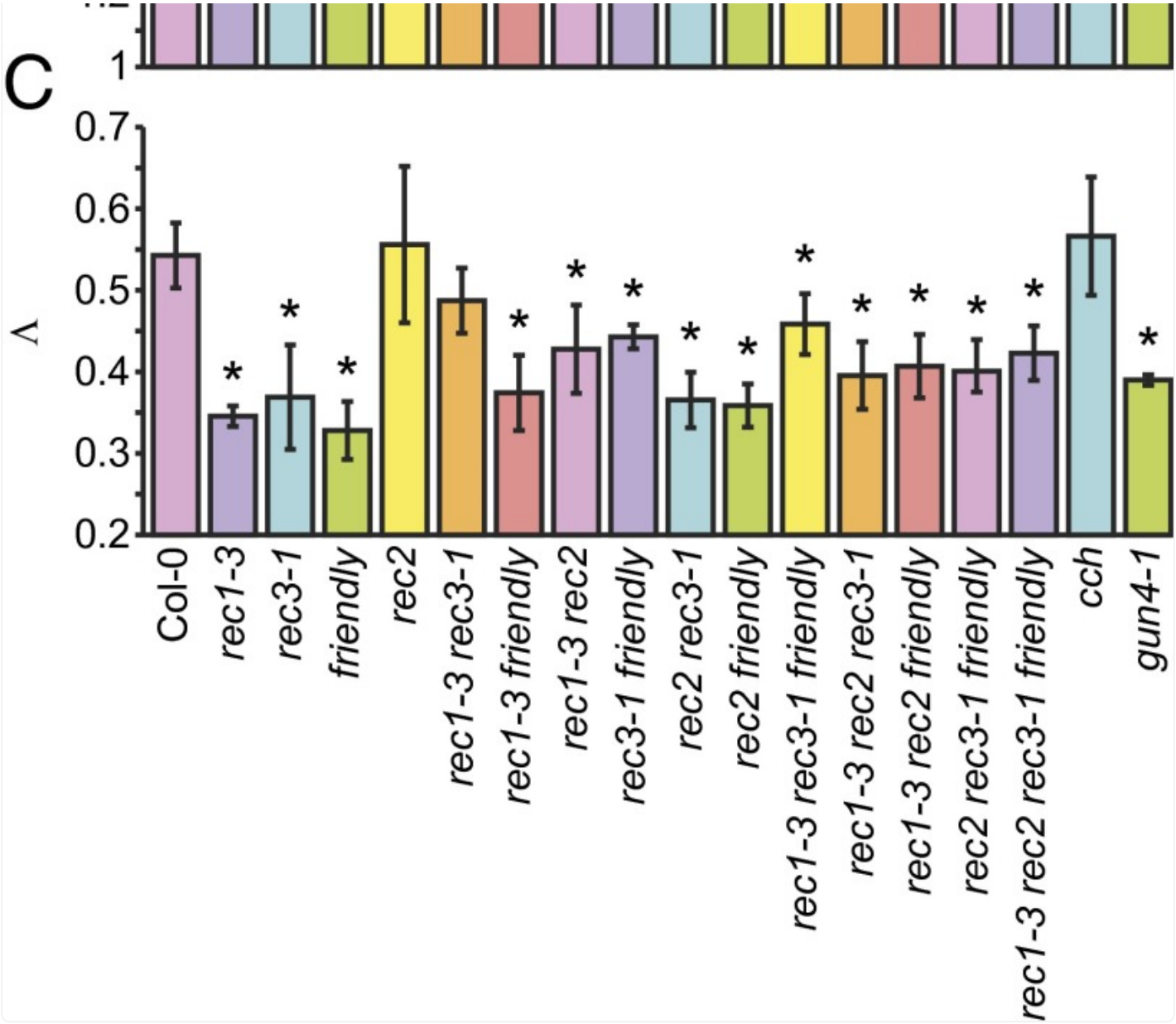

Open in a new tab

Live-cell imaging analysis of the chloroplasts from the *REC* gene family mutants. (*A*) Confocal laser scanning microscopy analysis of chloroplasts from the *REC* gene family mutants, *cch*, and *gun4-1*. Plants were grown on soil for 24 d. Each representative image was obtained by Z stacking 20 images from the abaxial surface of the leaf beginning in the epidermis and ending in the cortical region of the spongy mesophyll. (Scale bar, 20 μm.) (*B*) Fractal dimensions of the *REC* gene family mutants. Values of D_F were calculated from five to seven representative images to compare the geometric complexity of the distribution of chloroplasts in wild type and each mutant. Plant growth was as in *A*. Error bars indicate 95% confidence intervals. The asterisk indicates a statistically significant difference relative to wild type (Col-0) ($P < 0.0001$–0.045). (*C*) Lacunarity parameters of the *REC* gene family mutants. Values of Λ were calculated from five to seven representative images to compare the gaps in the distribution of chloroplasts in wild type and each mutant. Plant growth, error bars, and asterisk definition were as in *B* ($P < 0.0001$–0.02).

The chlorophyll biosynthesis mutants *cch* and *gun4-1* (29, 30) were analyzed to test whether chlorophyll deficiencies might cause similar phenotypes. *cch* and *gun4-1* were previously reported to accumulate only 30–40% of the chlorophyll found in wild type (30). Similar to the *REC* gene family mutants, the chloroplasts of *cch* and *gun4-1* appeared along the anticlinal walls in mesophyll cells (Fig. 3*A*), which is consistent with the enhanced sensitivities of chlorophyll-deficient mutants to light (31). *cch* exhibited enhanced chlorophyll fluorescence relative to *gun4-1* and wild type (*SI Appendix*, Fig. S15). Thus, chlorophyll deficiencies were not correlated with increases in chlorophyll fluorescence.

The distribution of chloroplasts within the mesophyll cells in many of these mutants appeared to differ from wild type (Fig. 3*A*). To quantify these differences, we calculated a fractal dimension (D_F) and a lacunarity parameter (Λ) for each image (32). Calculating D_F allowed us to compare the geometric complexity of the distribution of chloroplasts in wild type and each mutant (32). Calculating Λ allowed us to compare the heterogeneity (e.g., the gaps) in the distribution of chloroplasts in wild type and each mutant (32). Significant differences in the value of the D_F were observed in nine of these mutants (Fig. 3*B*). The values for D_F were not significantly different from wild type in *rec1-3*, *rec1-3 rec3-1*, and mutants containing both *rec3-1* and *friendly*, namely *rec3-1 friendly*, *rec1-3 rec3-1 friendly*, and *rec2 rec3-1 friendly* (Fig. 3*B*). In contrast to other mutants containing both *rec3-1* and *friendly*, the D_F of *rec1-3 rec2 rec3-1 friendly* was significantly less than wild type (Fig. 3*B*). This difference may reflect the decrease in the number of the chloroplasts in *rec1-3 rec2 rec3-1 friendly* relative to other mutants that contain both *rec3-1* and *friendly* (Fig. 3*A*). Chlorophyll deficiencies do not explain the differences in geometric complexities of these images because although the D_F values of the images from *cch* were significantly less than wild type, the D_F values of the images from *gun4-1* were not significantly different from wild type (Fig. 3*B*).

Λ was significantly reduced in all of the mutants except *rec2* and *rec1-3 rec3-1* (Fig. 3*C*). Although Λ was significantly less in *gun4-1* than in wild type, Λ was not significantly different between *cch* and wild type (Fig. 3*C*). Based on these data, we conclude that significant differences in the gaps of the chloroplast networks of the *rec* and *friendly* mutants were not caused by chlorophyll deficiencies. Our analysis of D_F and Λ provides evidence that the *rec* alleles, *friendly*, and combinations of the *rec* and *friendly* alleles affect the distribution of chloroplasts. Differences in the numbers, sizes, and shapes of these chloroplasts may account for some of these differences in D_F and Λ.

Mutants with abnormal distributions of chloroplasts often exhibit abnormal chloroplast movements because of deficiencies in the machinery that helps chloroplasts track along the cytoskeleton. Abnormal chloroplast movements are readily detected with chloroplast photorelocation experiments (27). We found that chloroplast photorelocation was indistinguishable between *rec1-3 rec2 rec3-1 friendly* and wild type (*SI Appendix*, Fig. S17 and Movies S1 and S2). We also imaged stromules by targeting yellow fluorescent protein (YFP) to the plastids because the number of stromules is reduced when the association of stromules and the cytoskeleton is disrupted (33). We observed no significant differences in the appearance or number of stromules in wild type, *rec1-3*, and *rec1-3 rec2 rec3-1* ($P = 0.1–0.5$) (*SI Appendix*, Fig. S18).

To quantify the reduced chloroplast compartment size phenotypes that we observed in live cells from the cortical region of the spongy mesophyll, we fixed leaf sections with glutaraldehyde and quantified the plan areas of fixed mesophyll cells and their chloroplasts (3). In the mutants, the size of the chloroplast compartment in the glutaraldehyde-fixed cells appeared reduced relative to wild type, especially in particular triple mutants and the quadruple mutant (Fig. 4*A*). The number of chloroplasts was correlated with the mesophyll cell plan area in each mutant and wild type (*SI Appendix*, Fig. S19). This correlation was previously demonstrated for wild type (2, 3, 7). We found that in many of the mutants, the number of chloroplasts per cell plan area was reduced relative to wild type. The greatest reductions in the number of chloroplasts per cell plan area were 44–62%, observed in *rec1-3 rec2*, *rec1-3 rec2 friendly*, *rec1-3 rec2 rec3-1*, and *rec1-3 rec2 rec3-1 friendly* (Fig. 4*B* and *SI Appendix*, Fig. S19). The reductions in the number of chloroplasts per cell plan area exhibited by *rec1-3 rec3-1* and *rec1-3 rec3-1 friendly* (24–25%) were significantly greater than in the relevant single mutants ($P < 0.0001$–0.03) (Fig. 4*B*). Without *rec1-3*, combinations of *rec2*, *rec3-1*, and *friendly* did not significantly decrease the number of chloroplasts per cell plan area. In most instances, *friendly* did not significantly affect the number of chloroplasts per cell plan area ($P = 0.0714$–0.9198). However, a significant increase in the number of chloroplasts per cell plan area was observed in *rec2 rec3-1 friendly* relative to *rec2 rec3-1* ($P = 0.0003$). Based on these data, we conclude that *rec1-3* attenuates the number of chloroplasts per cell plan area more than the other mutant alleles tested and that *friendly* promotes the number of chloroplasts per cell plan area in a specific genetic context.

Fig. 4.

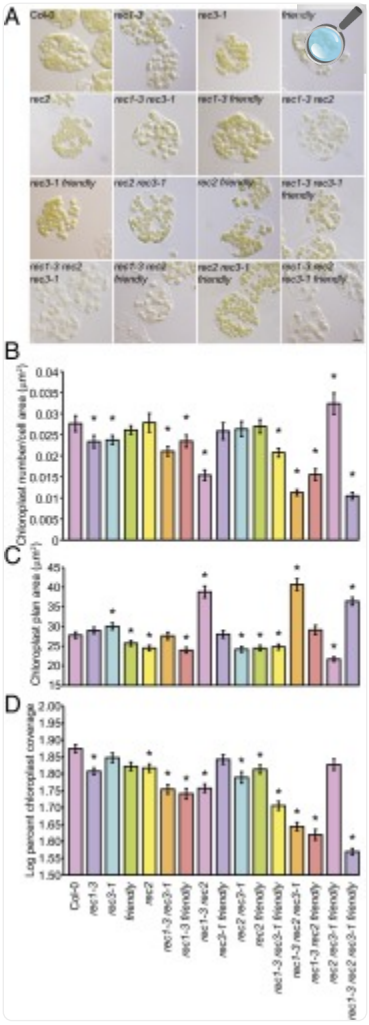

Open in a new tab

Glutaraldehyde-fixed mesophyll cells from the *REC* gene family mutants. (*A*) Representative differential interference contrast micrographs. Plants were grown on soil for 22 d. Glutaraldehyde-fixed mesophyll cells were visualized using differential interference contrast microscopy. Representative cells are shown. (Scale bar, 10 µm.) (*B*) Chloroplast number per cell plan area phenotypes. Plant growth was as in *A*. Error bars indicate 95% confidence intervals. The asterisk indicates a statistically significant difference relative to wild type (Col-0) ($P < 0.0001–0.004$). (*C*) Plan area phenotypes of individual chloroplasts. Plant growth, error bars, and asterisk definition are as in *B* ($P < 0.0001–0.0005$). (*D*) Chloroplast coverage phenotypes. Plant growth was as in *B*. A log transformation of the percent chloroplast coverage is presented. Error bars represent SEM. The asterisk indicates a statistically significant difference relative to wild type (Col-0) ($P < 0.0001–0.02$).

The mutants with no or small (15–25%) reductions in the number of chloroplasts per cell plan area also exhibited small (7–14%) reductions in chloroplast plan area relative to wild type (Fig. 4*C*). The largest reduction in chloroplast plan area was 22% observed in *rec2 rec3-1 friendly*. However, *rec2 rec3-1 friendly* was unusual relative to the other mutants tested in that it also exhibited a 17% increase in the number of chloroplasts per cell plan area relative to wild type (Fig. 4*B*). In contrast to the other mutants, the three most chlorophyll-deficient *REC* gene family mutants (*rec1-3 rec2*, *rec1-3 rec2 rec3-1*, and *rec1-3 rec2 rec3-1 friendly*; Fig. 2) exhibited 31–46% increases in their chloroplast plan areas relative to wild type (Fig. 4*C*). The increases in chloroplast plan area observed in *rec1-3 rec2*, *rec1-3 rec2 rec3-1*, and *rec1-3 rec2 rec3-1 friendly* are small compared with the 500% to ∼2,000% enlargements in chloroplast plan area that were reported for chloroplast division mutants (2, 5, 34). These findings are consistent with the idea that *rec* and *friendly* alleles disrupt mechanisms that regulate chloroplast division rather than those that perform chloroplast division. Numerous signals appear to regulate chloroplast division (2).

Consistent with the observed large reductions in the number of chloroplasts per cell plan area and either no increases or small increases in chloroplast plan area, we found that chloroplast coverage (total chloroplast plan area per cell plan area) was significantly reduced in many of the mutants compared with wild type (Fig. 4*D* and *SI Appendix*, Fig. S20). Moreover, we observed a significant interaction between the presence of *rec1-3* and the number of mutant alleles ($P < 0.00001$). In the presence of *rec1-3*, chloroplast coverage fell as the number of mutant alleles increased (Fig. 4*D*). The greatest reduction in chloroplast coverage (50%) was observed in the quadruple mutant (Fig. 4*D*).

In contrast, when plants contained *REC1*, adding further mutant alleles did not significantly reduce chloroplast coverage, regardless of the number of mutant alleles present (Fig. 4*D*).

Normalizing chlorophyll levels (Fig. 2) to chloroplast coverage (Fig. 4*D*) indicates that the chloroplasts of *friendly* accumulated significantly more chlorophyll than wild type (*SI Appendix*, Fig. S21). This analysis also indicates that the reduced chloroplast coverage phenotypes explain the chlorophyll-deficient phenotypes in *rec2*, *rec2 rec3-1*, *rec2 friendly*, and *rec2 rec3-1 friendly* and the differences between the severely chlorophyll-deficient mutants *rec1-3 rec2* and *rec1-3 rec2 rec3-1* and between *rec1-3 rec2 rec3-1* and *rec1-3 rec2 rec3-1 friendly* (*SI Appendix*, Fig. S21). However, normalizing chlorophyll levels to chloroplast coverage does not explain the chlorophyll-deficient phenotypes of *rec1-3*, the double and triple mutants that contain *rec1-3*, or the quadruple mutant (*SI Appendix*, Fig. S21). Thus, *rec1-3* attenuates both chloroplast coverage and the accumulation of chlorophyll.

To test whether chlorophyll deficiencies might contribute to these chloroplast coverage phenotypes, we analyzed glutaraldehyde-fixed mesophyll cells from *rec1-3 rec2 rec3-1 friendly*, *gun4-1*, and *cch* grown in 35 $\mu mol \cdot m^{-2} \cdot s^{-1}$ white light rather than the 125 $\mu mol \cdot m^{-2} \cdot s^{-1}$ white light that was used for the previous experiments. Reducing the irradiance increases chlorophyll levels in chlorophyll-deficient mutants (31). When grown in 125 $\mu mol \cdot m^{-2} \cdot s^{-1}$ white light, the individual chloroplasts of *cch* were difficult to distinguish by differential interference contrast microscopy. We also analyzed the glutaraldehyde-fixed mesophyll cells from four mutants grown in 125 $\mu mol \cdot m^{-2} \cdot s^{-1}$ white light: the

plastid-to-nucleus signaling mutant *gun1-101* (12) and the chlorophyll-deficient and photomorphogenic mutants *constitutive photomorphogenic 1-4* (*cop1-4*), *de-etiolated 1-1* (*det1-1*), and *phytochrome A phytochrome B* double mutant (*phyA phyB*) (35).

We found that *rec1-3 rec2 rec3-1 friendly* accumulated more than twofold higher levels of chlorophyll in 35 $\mu mol \cdot m^{-2} \cdot s^{-1}$ white light relative to 125 $\mu mol \cdot m^{-2} \cdot s^{-1}$ white light (*SI Appendix*, Fig. S22 *C* and *D*) and that *rec1-3 rec2 rec3-1 friendly*, *gun4-1*, *cch*, *cop1-4*, *det1-1*, and *phyA phyB* were chlorophyll-deficient relative to wild type (*SI Appendix*, Figs. S22 *C* and *D*, S23 *A*, *D*, and *E*, S24, and S25 *C* and *D*). The average number of chloroplasts per cell plan area decreased and the average chloroplast plan area increased in *rec1-3 rec2 rec3-1 friendly* and wild type in 35 $\mu mol \cdot m^{-2} \cdot s^{-1}$ white light relative to 125 $\mu mol \cdot m^{-2} \cdot s^{-1}$ white light (*SI Appendix*, Fig. S22 *A*, *E*, and *F*). We observed a variety of significant differences in the number of chloroplasts per cell plan area and chloroplast plan area phenotypes of *gun4-1*, *cch*, *cop1-4*, *det1-1*, and *phyA phyB* relative to wild type (*SI Appendix*, Figs. S23 *B*, *D*, *F*, and *G* and S25 *A*, *B*, *E*, and *F*). The more than twofold increase in chlorophyll levels did not affect chloroplast coverage in *rec1-3 rec2 rec3-1 friendly* (*SI Appendix*, Fig. S22 *B* and *G*). Chloroplast coverage was not significantly different from wild type in *gun4-1*, *cch*, *cop1-4*, *det1-1*, or *phyA phyB* ($P = 0.7–1.0$) (*SI Appendix*, Figs. S23 *C*, *D*, and *H* and S25 *B* and *G*). The number of chloroplasts per cell plan area, chloroplast plan area, and chloroplast coverage phenotypes of *gun1-101* were not significantly different from wild type ($P = 0.6–0.8$) (*SI Appendix*, Fig. S26).

We conclude that both the number of chloroplasts per cell plan area and chloroplast plan area are probably controlled by a number of mechanisms that regulate chloroplast division, and that these signals include light signaling and signals induced by chlorophyll deficiencies. Chlorophyll deficiencies do not completely explain these phenotypes because, although the chloroplast plan areas were larger than wild type in *cop1-4*, *det1-1*, *phyA phyB*, *rec1-3 rec2*, *rec1-3 rec2 rec3-1*, and *rec1-3 rec2 rec3-1 friendly*, the chloroplast plan areas were smaller than wild type in *cch* and *gun4-1*. Additionally, we conclude that, in general, altering light-regulated development and significantly attenuating the accumulation of chlorophyll do not affect chloroplast coverage in *Arabidopsis* mesophyll cells. We also conclude that chlorophyll deficiencies do not explain the reduced chloroplast coverage phenotypes of the *rec* mutants.

We found that two components of the chloroplast division machinery—filamenting temperature-sensitive Z (FtsZ)1-1 and FtsZ2-1—accumulated to lower levels in *rec1-3 rec2 rec3-1 friendly* than in wild type (*SI Appendix*, Fig. S27). Reducing the levels of FtsZ1-1 and FtsZ2-1 inhibits chloroplast division but does not affect chloroplast coverage (36). Any number of signals may down-regulate the expression of FtsZ1-1 and Fts2-1 in *rec1-3 rec2 rec3-1 friendly*. The reduced expression of FtsZ1-1 and Fts2-1 may partially explain the enlarged chloroplasts of *rec1-3 rec2 rec3-1 friendly*.

To test whether the levels of the REC1 protein limit the size of the chloroplast compartment, we used the 35S promoter from cauliflower mosaic virus to drive the overexpression of *REC1* in *sgs3 rdr6-11*—a double mutant that is resistant to transgene-induced gene silencing (37). We found three independent transgenic lines that accumulated more REC1 protein than *sgs3 rdr6-11* (*SI Appendix*, Fig. S28). Chloroplast coverage increased from 11% to 17% in the transgenic

lines that accumulated elevated levels of REC1 (Fig. 5*A* and *SI Appendix*, Fig. S29). In lines 40 and 66, the increase in chloroplast coverage appeared to result mostly from an increase in the number of chloroplasts per cell plan area without a significant change in the plan areas of individual chloroplasts (Fig. 5*B*). However, plots of total chloroplast plan area and chloroplast number versus cell plan area provide evidence for heterogeneity in the organellar basis for the increase in chloroplast coverage for line 40 (*SI Appendix*, Fig. S29), possibly resulting from the attenuation of chloroplast division in some of the larger cells from line 40. In line 44, the increase in chloroplast coverage appeared to result from an increase in the plan areas of individual chloroplasts and no change in the number of chloroplasts per cell (Fig. 5*C* and *SI Appendix*, Fig. S29), possibly resulting from the misregulation of chloroplast division in this particular transgenic plant.

Fig. 5.

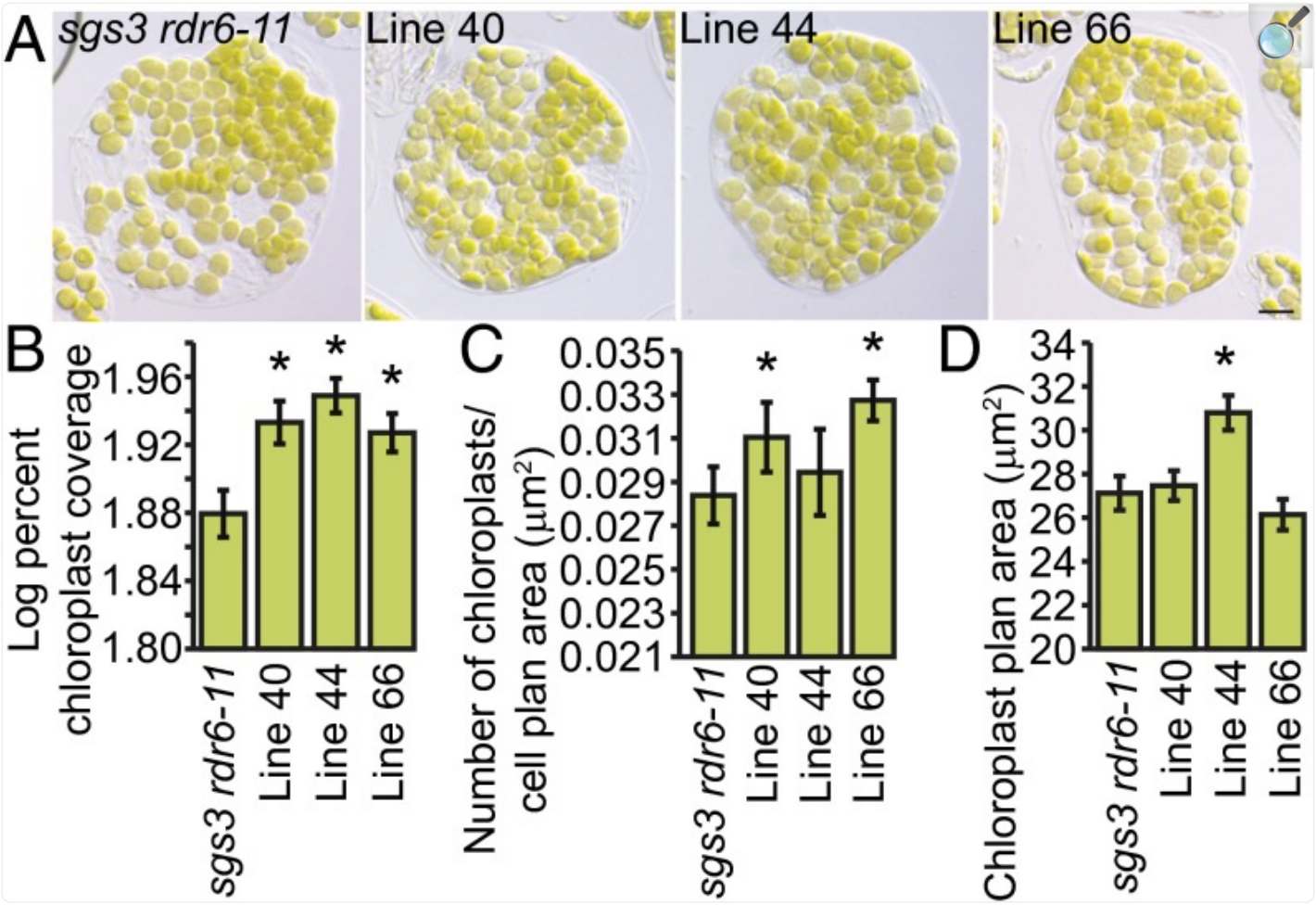

Open in a new tab

Analysis of glutaraldehyde-fixed mesophyll cells from *sgs3 rdr6-11* lines overexpressing *REC1*. (*A*) Glutaraldehyde-fixed cells. Plants were grown on soil for 24 d. Representative cells from wild type and plants 40, 44, and 66 that overexpress *REC1* are shown. (Scale bar, 10 μm.) (*B*) Chloroplast coverage phenotypes of *sgs3 rdr6-11* and *sgs3 rdr6-11* lines overexpressing *REC1*. A log transformation of the percent chloroplast coverage is presented. Error bars represent SEM. The asterisk indicates a statistically significant difference relative to *sgs3 rdr6-11* ($P = 0.0005–0.02$). (*C*) Chloroplast number per cell plan area phenotypes of *sgs3 rdr6-11* and *sgs3 rdr6-11* lines overexpressing *REC1*. Error bars indicate 95% confidence intervals. The asterisk definition is as in *B* ($P = 0.0006$ and 0.02). (*D*) Plan area phenotypes of individual chloroplasts from *sgs3 rdr6-11* and *sgs3 rdr6-11* lines overexpressing *REC1*. Error bars and asterisk definition are as in *C* ($P < 0.0001$).

Subcellular Distribution of REC1.

To gain insight into the mechanism that underpins the biological functions of REC1, we determined the subcellular distribution of REC1 by fusing YFP to the carboxyl terminus of REC1, transiently expressing the REC1-YFP fusion protein in tobacco leaves and monitoring the subcellular distribution of REC1-YFP by confocal laser scanning microscopy. To test whether REC1-YFP was transiently expressed as a full-length protein, we analyzed leaf sections expressing REC1-YFP by immunoblotting with anti-GFP antibodies. The immunoblotting analysis indicates that REC1-YFP accumulates as a single band (*SI Appendix*, Fig. S30*A*) and that the mass of REC1-YFP is greater than the mass of native REC1 (*SI Appendix*, Figs. S3*D* and S30*B*).

Live-cell confocal microscopy analyses with settings that distinguish GFP, YFP, and chlorophylls (38) show REC1-YFP in the nucleus and the cytosol (Fig. 6*A*). The nucleus is recognizable by the appearance of the nucleolus (Fig. 6*A*, arrow) and by the localization of ssGFP-HDEL, an endoplasmic reticulum marker that defines the nuclear envelope (39) (Fig. 6*B*). We found that REC1-YFP is excluded from chloroplasts (Fig. 6 *C* and *D*).

Fig. 6.

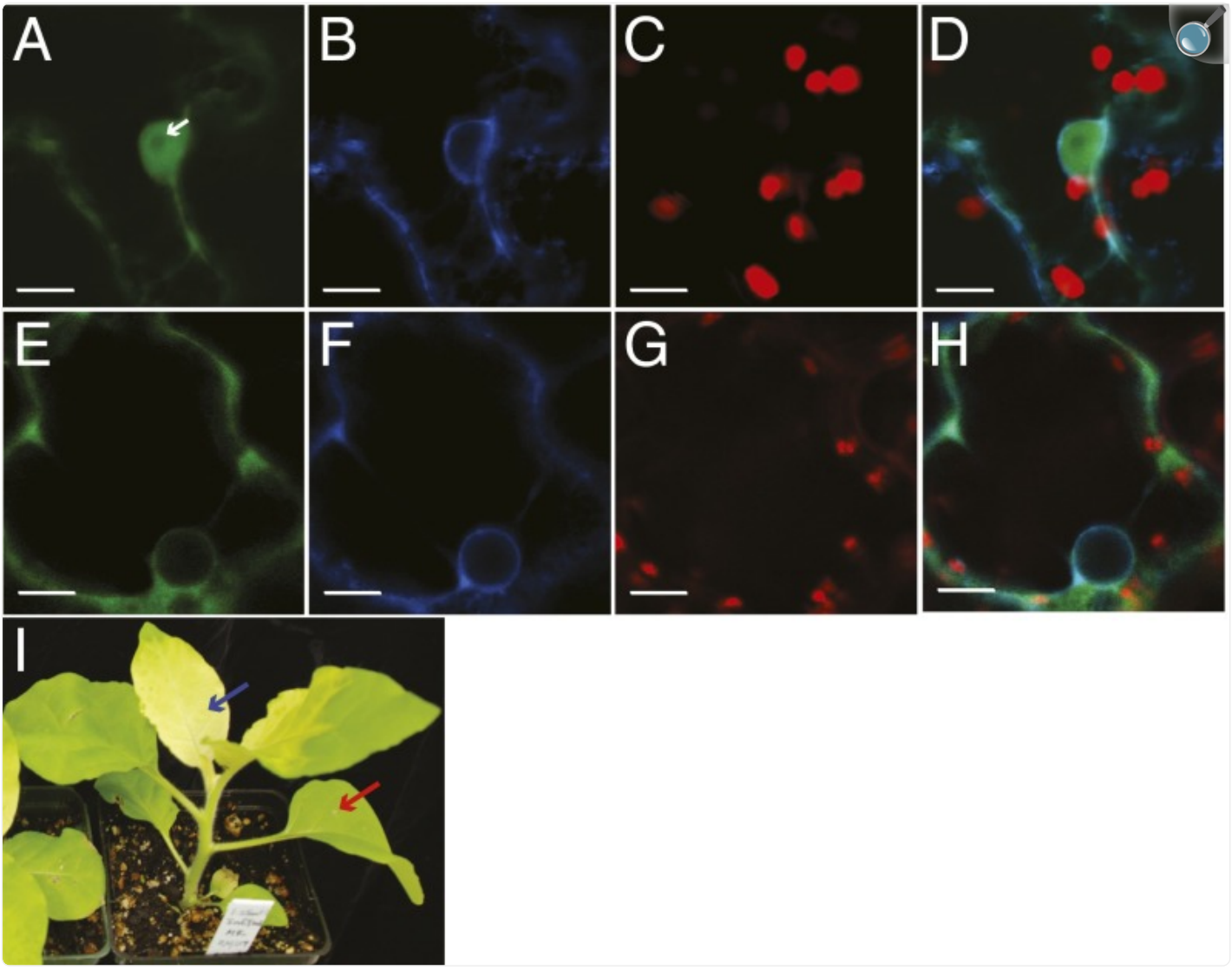

Open in a new tab

Subcellular distribution of REC1-YFP in herbicide-treated and untreated leaf cells. Micrographs of untreated tobacco cells (*A–D*) and amitrole-treated tobacco cells (*E–H*): REC1-YFP (*A* and *E*), HDEL-GFP (*B* and *F*), chlorophyll fluorescence (*C* and *G*), and merged images (*D* and *H*). (Scale bars, 10 μm.) (*I*) Representative tobacco plant 10 d after amitrole treatment. The red arrow indicates the leaf infiltrated with amitrole. The blue arrow indicates the site of coinfiltration with REC1-YFP and HDEL-GFP.

To test whether the functional state of the chloroplast might affect the subcellular distribution of REC1, we infiltrated one leaf of a tobacco plant with amitrole, an herbicide that causes chlorophyll deficiencies (40). We found that amitrole

caused observable chlorophyll deficiencies in leaves that developed from shoot apical meristems after infiltrations (Fig. 6*I*). We suggest that amitrole moved from the sites of infiltrations to the shoot apical meristem, where it attenuated the chloroplast biogenesis that occurred during leaf development. In these chlorophyll-deficient leaves, chloroplasts were significantly smaller than in untreated leaves (Fig. 6 *C* and *G*). In these chlorophyll-deficient leaves, REC1-YFP localized to the cytosol and was excluded from the nucleus (Fig. 6 *E–H*).

We tested whether REC1 was enriched in nuclear and cytosolic fractions prepared from *Arabidopsis* seedlings. The enrichment of histone H3 and UDP glucose pyrophosphorylase in the nuclear and cytosolic fractions, respectively, indicates that nuclei and cytosols were enriched in these preparations (Fig. 7*A*). Using affinity-purified anti-REC1 antibodies (*SI Appendix*, Fig. S3), we found that REC1 was enriched in these nuclear and cytosolic fractions (Fig. 7*A*). Although these anti-REC1 antibodies recognized multiple bands in the nuclear and cytosolic fractions, they recognized only one band in the whole-seedling extracts prepared using denaturing conditions (Fig. 7*A* and *SI Appendix*, Fig. S3*B*). We conclude that the affinity-purified anti-REC1 antibodies recognize multiple bands in the nuclear and cytosolic fractions, because partial proteolysis of REC1 occurred during the purification of the nuclear and cytosolic fractions. Next, we tested whether herbicides affect the levels of REC1 in purified nuclei. We found that REC1 was present at similar levels in nuclei regardless of whether nuclei were purified from untreated seedlings or seedlings that lacked functional chloroplasts because chloroplast biogenesis was blocked with a norflurazon treatment (Fig. 7 *A* and *B* and *SI Appendix*, Fig. S31*A*). When chloroplast biogenesis was blocked with an amitrole treatment, much longer exposures of immunoblots than used to detect REC1 in the nuclear fractions from norflurazon-treated and untreated seedlings provided evidence that only trace quantities of REC1 accumulated in nuclei purified from amitrole-treated seedlings (Fig. 7*B* and *SI Appendix*, Fig. S31*A*). Methyl viologen induces a rise in the levels of chloroplastic reactive oxygen species that causes chloroplast dysfunction and activates the plastid-to-nucleus signaling that induces the expression of nuclear genes, such as the nuclear genes that encode cytosolic ascorbate peroxidase (41). To test whether chloroplastic reactive oxygen species affect the nucleocytoplasmic partitioning of REC1, we transferred 5-d-old seedlings to a growth medium that contained 1 μM methyl viologen and allowed the seedlings to grow for an additional 3 d. Higher levels of cytosolic ascorbate peroxidase and lower levels of chlorophyll accumulated in the methyl viologen-treated seedlings than in untreated seedlings (*SI Appendix*, Fig. S31 *B–D*). We conclude that this methyl viologen treatment induced chloroplast dysfunction and the expression of cytosolic ascorbate peroxidase, probably by inducing a rise in the levels of chloroplastic reactive oxygen species. We found that REC1 accumulated to similar levels in the nuclei of methyl viologen-treated and untreated seedlings (Fig. 7*C*). In addition to inhibiting chloroplast function, amitrole inhibits root elongation (40), which depends on cell division and cell elongation (42). To test whether inhibiting cell expansion might drive REC1 out of the nucleus, we tested whether REC1 accumulates in the nuclei of the *Arabidopsis* null mutant *rhd3-7* (43). *rhd3-7* and other *RHD3* mutants are smaller than wild type because cell expansion is inhibited in these mutants (*SI Appendix*, Fig. S31*A*) (43, 44). We found that REC1 accumulated to similar levels in the nuclei of *rhd3-7* and wild type (Fig. 7*D*). We conclude that amitrole treatments specifically exclude REC1 from the nucleus.

Fig. 7.

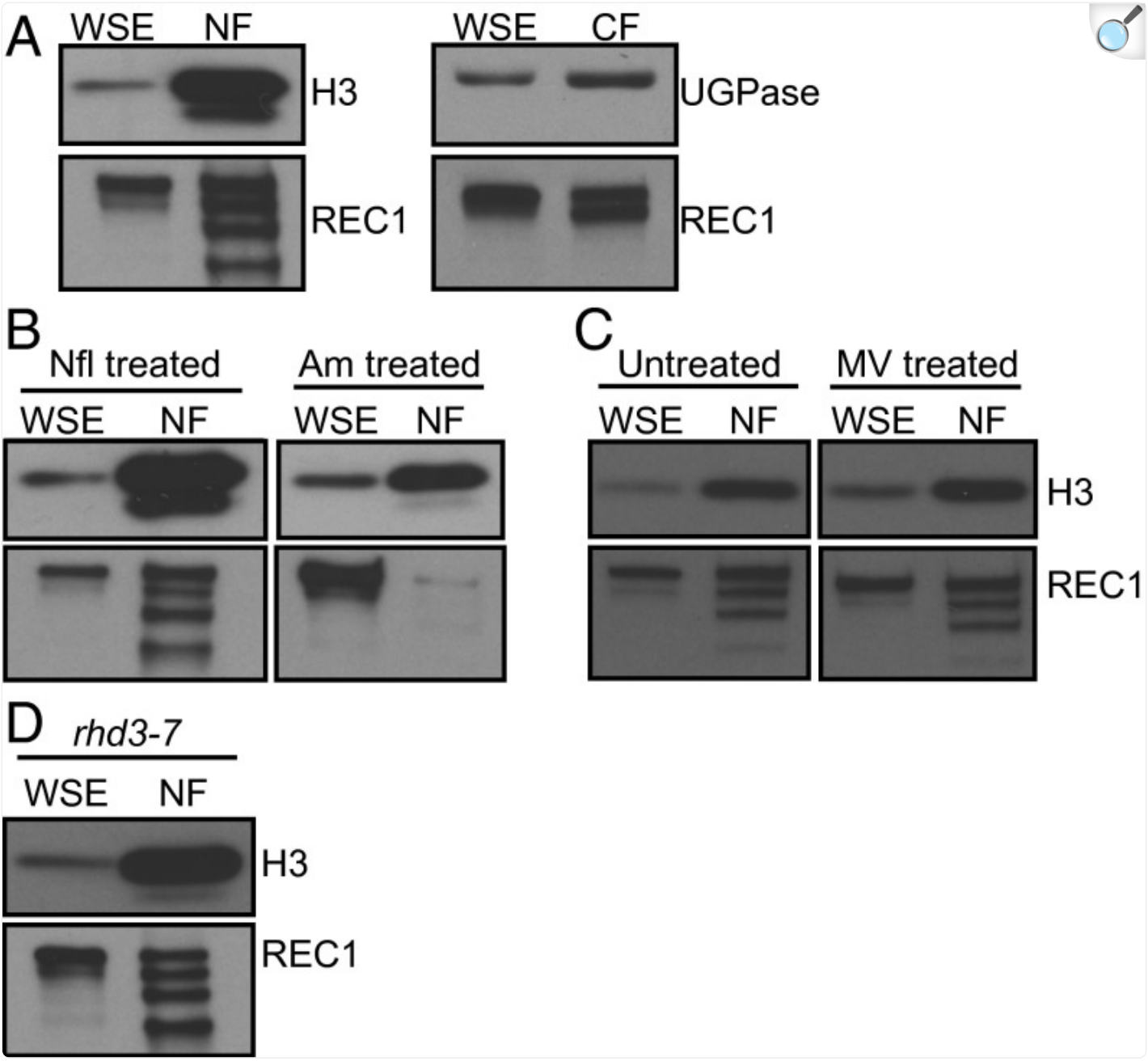

Open in a new tab

Subcellular distribution of REC1 in herbicide-treated and untreated seedlings. (*A*) Subcellular distribution of REC1 in untreated seedlings. Whole-seedling extracts (WSE), nuclear fractions (NF), and cytosolic fractions (CF) were prepared from 8-d-old seedlings that were grown on LS medium that lacked an herbicide. Fractions were analyzed by immunoblotting with anti-histone H3 (H3), anti–UDP-glucose pyrophosphorylase (UGPase), and anti-REC1 (REC1) antibodies. Each lane contains 3 μg of protein. (*B*) Levels of REC1 in

nuclei purified from norflurazon-treated and amitrole-treated seedlings. Seedlings were grown for 8 d on LS medium that contained either norflurazon (Nfl-treated) or amitrole (Am-treated). Whole-seedling extracts and nuclear fractions were analyzed as in *A*. (*C*) Levels of REC1 in nuclei purified from methyl viologen-treated seedlings. Seedlings were grown for 8 d on LS medium (untreated) or seedlings were grown for 5 d on LS medium and then transferred to the same medium containing 1 μM methyl viologen for 3 d (MV-treated). Whole-seedling extracts and nuclear fractions were analyzed as in *A*. (*D*) Levels of REC1 in nuclei purified from *rhd3-7*. Plant growth and analysis of whole-seedling extracts and nuclear fractions were as in *A*.

Discussion

Our phenotypic characterizations provide evidence that the proteins encoded by the *REC* gene family link increases in mesophyll cell size to increases in chloroplast compartment size. Other than the proteins encoded by the *REC* gene family, there are no candidates for proteins that contribute to this mechanism (2, 6, 45).

Cells of the shoot apical meristem contain fewer than 10 proplastids. After chloroplast biogenesis and during the mesophyll cell expansion that occurs during leaf development, there is a large increase in the number of chloroplasts in mesophyll cells (45). The mesophyll cells from *rec1-3 rec2 rec3-1 friendly* contained 22 ± 8 chloroplasts (*SI Appendix*, Figs. S19 and S22*A*). Thus, the mechanism that establishes the size of the chloroplast compartment is partially active in *rec1-3 rec2 rec3-1 friendly*. A few models are consistent with these data. One possibility is that the proteins encoded by the *REC* gene family directly contribute to the mechanism that establishes the size of the chloroplast compartment and that this mechanism retains partial activity in *rec1-3 rec2 rec3-1 friendly*. Another possibility is that the proteins encoded by the *REC* gene family regulate a mechanism that establishes the size of the chloroplast compartment. A third possibility is that the proteins encoded by the *REC* gene family contribute to a mechanism that helps to establish the size of the chloroplast compartment, and a distinct mechanism that does not require the *REC* genes independently contributes to the size of the chloroplast compartment.

Further study of the *REC* genes may lead to the ability to rationally manipulate the size of the chloroplast compartment and to the engineering of C_4 photosynthesis into C_3 plants, which is anticipated to increase yields from important crops, such as rice (9, 11). The contribution of the *REC* genes to the distribution of chloroplasts in mesophyll cells may also contribute to the engineering of C_4 photosynthesis into C_3 plants, because the distribution of chloroplasts within mesophyll cells differs between C_3 and C_4 plants (11). The *rec* and *friendly* mutants appear deficient in a mechanism that is distinct from the mechanisms that are deficient in other chloroplast distribution mutants because in contrast to the normal photorelocation observed in *rec1-3 rec2 rec3-1 friendly*, the photorelocation of chloroplasts is abnormal in other chloroplast distribution mutants (27).

In contrast to the *rec2*, *rec3*, and *friendly* alleles that we tested, *rec1-3* reduces the accumulation of chlorophyll. This observation raised the possibility that the chlorophyll deficiencies of the *rec1* mutants might prevent chloroplasts from keeping pace with a mechanism that establishes the size of the chloroplast compartment. Indeed, in *crumpled leaf* (*crl*) and *clumped chloroplasts 1* (*clmp1*), chloroplasts do not keep pace with this mechanism because chloroplasts are not equally distributed between daughter cells during cell division (46, 47). Our finding that inducing an increase in the levels of chlorophyll does not affect chloroplast coverage in *rec1-3 rec2 rec3-1 friendly* and that chloroplast coverage is not significantly different from wild type in the chlorophyll-deficient mutants *cch*, *gun4-1*, *cop1-4*, *det1-1*, and *phyA phyB* indicates that chlorophyll deficiencies do not prevent chloroplasts from keeping pace with the mechanism that establishes the size of the chloroplast compartment. Chlorophyll deficiency is a common phenotype in *Arabidopsis*. Thus, disrupting any number of chloroplast functions may indirectly affect the thylakoid membranes. Indeed, disrupting mechanisms that drive chloroplast division and mechanisms that potentially regulate chloroplast division appears to indirectly affect the normal development of the thylakoid membranes (34, 48, 49) and the accumulation of chlorophyll (47, 50, 51).

The screening of 3,500 ethylmethanesulfonate (EMS) mutants for plants with aberrant morphologies in the chloroplast compartment, such as abnormal chloroplast coverage (3), was not sufficient to saturate this screen (52). Nonetheless, screening ∼2,000 EMS-mutagenized *Arabidopsis* plants is usually sufficient for isolating specific mutants (53). Indeed, the screen of Pyke and Leech (3) yielded more than 10 different genes that, in most instances, encode proteins that directly contribute to chloroplast division (2). An additional screen of 10,000 EMS mutants for plants with enlarged chloroplasts yielded only one additional gene that directly contributes to chloroplast division (54). Additionally, a screen of 5,200 *Arabidopsis* mutants that were homozygous for T-DNA insertions in nuclear genes that mostly encode chloroplast proteins for mutants with aberrant morphologies in the chloroplast compartment, such as abnormal chloroplast coverage, yielded one chloroplast division mutant and no chloroplast coverage mutants (46). These data and our finding that chloroplast coverage is not different from wild type in *cch*, *gun4-1*, *gun1-101*, *cop1-4*, *det1-1*, and *phyA phyB* indicate that a reduction in the size of the chloroplast compartment is not a common phenotype. We suggest that the *REC* genes may directly contribute to a mechanism that links increases in the size of the chloroplast compartment to increases in the size of mesophyll cells because reduced chloroplast coverage is not a common phenotype and because overexpressing REC1 induces significant increases in chloroplast coverage. Our finding that the REC1 protein resides in the cytosol and nucleus further supports the idea that REC1 helps to establish the size of the chloroplast compartment because this mechanism is expected to reside in an extraplastidic compartment.

A less than twofold increase in chloroplast coverage was observed in the fully expanded leaves and mature green fruits of the *high pigment 1* (*hp-1*) mutant of tomato (55). *HP-1* encodes UV-damaged DNA-binding protein 1 (DDB1) (56). DDB1 interacts with DET1, a master repressor of light-regulated development that contributes to ubiquitin-proteasome–mediated protein degradation (35). Our analysis of *cop1-4*, *det1-1*, and *phyA phyB* indicates that defects in light-regulated development do not necessarily affect the size of the chloroplast compartment in mesophyll cells.

The biochemical functions of REC1, REC2, and REC3 are not known. FRIENDLY appears to perform a variety of functions (13, 20, 21). The indistinguishable photorelocation of chloroplasts that we observed in wild type and *rec1-3 rec2 rec3-1 friendly* and the localization of REC1 to both the cytosol and the nucleus conflict with the idea that REC proteins directly contribute to the tracking of chloroplasts along the cytoskeleton. Similarly, mitochondrial clustering in *friendly* does not result from a cytoskeletal or motor defect (13). The enhanced chlorophyll fluorescence, chloroplasts aligning along the anticlinal walls, abnormal chloroplast ultrastructure, and chlorophyll deficiencies in the *rec* and *friendly* mutants indicate that these mutant alleles induce chloroplast dysfunction. REC1, REC2, REC3, and FRIENDLY may contribute to processes in the cytosol and nucleus that promote the function of chloroplasts and mitochondria. Consistent with this interpretation, FRIENDLY was localized to the cytosol, and mutations in *FRIENDLY* and the *Drosophila* ortholog of *FRIENDLY* induce metabolic dysfunction (13, 57).

The finding that REC1 is excluded from the nucleus when chloroplast biogenesis is blocked or attenuated with an amitrole treatment is consistent with a plastid signaling mechanism that is activated by amitrole treatments regulating the subcellular distribution of REC1. This inference follows because proteins larger than ∼40 kDa are actively transported across the nuclear envelope (58) and because the nucleocytoplasmic partitioning of proteins contributes to a number of processes, including diverse signaling mechanisms (35, 58). The finding that, in contrast to amitrole treatments, norflurazon and methyl viologen treatments do not exclude REC1 from the nucleus is consistent with a plastid signaling mechanism that is activated by amitrole treatments but not activated by norflurazon and methyl viologen treatments regulating the subcellular distribution of REC1. Consistent with this interpretation, plastid-to-nucleus signaling mechanisms appear numerous (8).

Another possibility is that an extraplastidic mechanism that is inhibited by amitrole treatments might affect the subcellular distribution of REC1 because in contrast to norflurazon and methyl viologen (8, 59), amitrole is not a specific inhibitor of chloroplast function. Although amitrole inhibits plastidic processes, such as carotenoid biosynthesis and histidine biosynthesis, amitrole is more effective at inhibiting root elongation, which depends on cell division and cell elongation (40). Our findings that the *REC* genes link increases in cell size to increases in chloroplast compartment size and that amitrole specifically affects the nucleocytoplasmic partitioning of REC1 are consistent with the inhibition of cell expansion regulating the subcellular distribution of REC1. If the inhibition of cell expansion excludes REC1 from the nucleus, *rhd3-7* may not affect the nucleocytoplasmic partitioning of REC1 because *rhd3-7* does not sufficiently inhibit cell expansion.

Amitrole treatments may inhibit a process in the nucleus by excluding REC1 from the nucleus. Alternatively, amitrole-treated plants may attempt to stimulate a cytosolic process by driving REC1 into the cytosol. Another possibility is that REC1 performs the same function or different functions in the nucleus and the cytosol.

In summary, we provide evidence that *REC1*, *REC2*, *REC3*, and *FRIENDLY* promote the proper morphology, function, and size of the chloroplast compartment. These functions may depend on the trafficking of REC1 between the nucleus

and the cytosol. Signals activated by the inhibition of cell expansion or chloroplast dysfunction may regulate this mechanism. Understanding the biochemical function of REC1 and the nucleocytoplasmic partitioning of REC1 may lead to the rational manipulation of the size of the chloroplast compartment and higher yields from important crops.

Materials and Methods

Detailed information on the materials and methods used in this study is provided in *SI Appendix*.

Plant Materials and Growth Conditions.

All mutants used in this study were derived from *A. thaliana* ecotype Columbia-0 (Col-0). Plants were grown on soil or on Linsmaier and Skoog (LS) growth medium in either broad-spectrum white light or far-red light in controlled-environment chambers. The far-red block of greening experiments were adapted from Barnes et al. (15).

Analysis of Chlorophylls.

Chlorophylls were extracted using *N*,*N*′-dimethylformamide and quantified by spectrophotometry.

Analysis of Chloroplasts by Microscopy.

Chloroplasts were imaged by confocal laser scanning microscopy. Chlorophyll fluorescence, D_F, and Λ were calculated from maximum-intensity projection images built from Z-stack images. The chloroplast number per cell plan area, chloroplast plan area, and chloroplast coverage were quantified as described previously (3).

Construction, Expression, and Imaging of the REC1-YFP Fusion Gene.

The ORF that encodes YFP was fused in-frame and downstream of an ORF that encodes the full-length REC1. Transient expression of REC1-YFP in *Nicotiana tabacum* was performed by infiltrating amitrole-treated or untreated leaves with an *Agrobacterium tumefaciens* strain harboring the REC1-YFP fusion gene. The imaging of YFP fluorescence was performed using confocal laser scanning confocal microscopes.

Analysis of Whole-Seedling Extracts, Nuclear Fractions, and Cytosolic Fractions.

Seedlings were grown on LS medium containing no sucrose or on the same medium containing 1% sucrose and an herbicide. Whole-seedling extracts were prepared by boiling frozen and powdered seedlings in SDS/PAGE sample

buffer and then clarifying these extracts by centrifugation at 16,000 × *g* for 10 min. Nuclei were purified from seedlings using Percoll step gradients. Cytosolic fractions were the supernatants that were obtained by lysing purified protoplasts and then clarifying these lysates by centrifugation at 21,000 × *g* for 15 min. Equal amounts of protein were analyzed by immunoblotting.

Supplementary Material

Supplementary File

pnas.1515741113.sapp.pdf (33.7MB, pdf)

Supplementary File

Download video file (704.1KB, avi)

Supplementary File

Download video file (484.4KB, avi)

Acknowledgments

We thank Dean DellaPenna (Michigan State University) for providing the recombinant inbred lines CL67, CL35, and CL115. We thank Alicia Pastor at the Center for Advanced Microscopy (Michigan State University) for assistance with the transmission electron microscopy experiments, Neil Adhikari (Michigan State University) for *sgs3 rdr6-11*, and Lauren A. Lawrence (Michigan State University) for technical assistance. R.M.L. thanks members of the K.W.O. laboratory, especially Deena Kadirjan-Kalbach and Allan TerBush, for many helpful discussions. This work was supported by National Science Foundation (NSF) Grants IOB 0517841 and IOS 1021755 (to R.M.L.); NSF Grant MCB-1121943 (to K.W.O.); NSF Grant MCB1243792 and NASA Grant NNX12AN71G (to F.B.); AgBioResearch (F.B.); and US Department of Energy, Office of Science, Basic Energy Sciences Grant DE-FG02-91ER20021 (to

R.M.L. and F.B.) and Grant DE-FG02-06ER15808 (to K.W.O.).

Footnotes

The authors declare no conflict of interest.

This article is a PNAS Direct Submission.

This article contains supporting information online at www.pnas.org/lookup/suppl/doi:10.1073/pnas.1515741113/-/DCSupplemental .

References

1. Pogson BJ, Ganguly D, Albrecht-Borth V. Insights into chloroplast biogenesis and development. Biochim Biophys Acta. 2015;1847(9):1017–1024. doi: 10.1016/j.bbabio.2015.02.003. [DOI] [PubMed] [Google Scholar]

2. Osteryoung KW, Pyke KA. Division and dynamic morphology of plastids. Annu Rev Plant Biol. 2014;65:443–472. doi: 10.1146/annurev-arplant-050213-035748. [DOI] [PubMed] [Google Scholar]

3. Pyke KA, Leech RM. Rapid image analysis screening procedure for identifying chloroplast number mutants in mesophyll cells of Arabidopsis thaliana (L.) Heynh. Plant Physiol. 1991;96(4):1193–1195. doi: 10.1104/pp.96.4.1193. [DOI] [PMC free article] [PubMed] [Google Scholar]

4. Pyke KA, Leech RM. Chloroplast division and expansion is radically altered by nuclear mutations in Arabidopsis thaliana. Plant Physiol. 1992;99(3):1005–1008. doi: 10.1104/pp.99.3.1005. [DOI] [PMC free article] [PubMed] [Google Scholar]

5. Pyke KA, Leech RM. A genetic analysis of chloroplast division and expansion in Arabidopsis thaliana. Plant Physiol. 1994;104(1):201–207. doi: 10.1104/pp.104.1.201. [DOI] [PMC free article] [PubMed] [Google Scholar]

6. Pyke KA. Plastid division and development. Plant Cell. 1999;11(4):549–556. doi: 10.1105/tpc.11.4.549. [DOI] [PMC free article] [PubMed] [Google Scholar]

7. Kawade K, Horiguchi G, Ishikawa N, Hirai MY, Tsukaya H. Promotion of chloroplast proliferation upon enhanced post-mitotic cell expansion in leaves. BMC Plant Biol. 2013;13:143. doi: 10.1186/1471-2229-13-143. [DOI] [PMC free article] [PubMed] [Google Scholar]

8. Larkin RM. Influence of plastids on light signalling and development. Philos Trans R Soc Lond B Biol Sci. 2014;369(1640):20130232. doi: 10.1098/rstb.2013.0232. [DOI] [PMC free article] [PubMed] [Google Scholar]

9. von Caemmerer S, Quick WP, Furbank RT. The development of C4 rice: Current progress and future challenges. Science. 2012;336(6089):1671–1672. doi: 10.1126/science.1220177. [DOI] [PubMed] [Google Scholar]

10. Sage RF, Khoshravesh R, Sage TL. From proto-Kranz to C4 Kranz: Building the bridge to C4 photosynthesis. J Exp Bot. 2014;65(13):3341–3356. doi: 10.1093/jxb/eru180. [DOI] [PubMed] [Google Scholar]

11. Stata M, et al. Mesophyll cells of C4 plants have fewer chloroplasts than those of closely related C3 plants. Plant Cell Environ. 2014;37(11):2587–2600. doi: 10.1111/pce.12331. [DOI] [PubMed] [Google Scholar]

12. Ruckle ME, DeMarco SM, Larkin RM. Plastid signals remodel light signaling networks and are essential for efficient chloroplast biogenesis in Arabidopsis. Plant Cell. 2007;19(12):3944–3960. doi: 10.1105/tpc.107.054312. [DOI] [PMC free article] [PubMed] [Google Scholar]

13. El Zawily AM, et al. FRIENDLY regulates mitochondrial distribution, fusion, and quality control in Arabidopsis. Plant Physiol. 2014;166(2):808–828. doi: 10.1104/pp.114.243824. [DOI] [PMC free article] [PubMed] [Google Scholar]

14. Terry MJ, Smith AG. A model for tetrapyrrole synthesis as the primary mechanism for plastid-to-nucleus signaling during chloroplast biogenesis. Front Plant Sci. 2013;4:14. doi: 10.3389/fpls.2013.00014. [DOI] [PMC free article] [PubMed] [Google Scholar]

15. Barnes SA, Nishizawa NK, Quaggio RB, Whitelam GC, Chua NH. Far-red light blocks greening of Arabidopsis seedlings via a phytochrome A-mediated change in plastid development. Plant Cell. 1996;8(4):601–615. doi: 10.1105/tpc.8.4.601. [DOI] [PMC free article] [PubMed] [Google Scholar]

16. Zeytuni N, Zarivach R. Structural and functional discussion of the tetra-trico-peptide repeat, a protein interaction module. Structure. 2012;20(3):397–405. doi: 10.1016/j.str.2012.01.006. [DOI] [PubMed] [Google Scholar]

17. Neumann CJ, Cohen SM. Sternopleural is a regulatory mutation of wingless with both dominant and recessive effects on larval development of Drosophila melanogaster. Genetics. 1996;142(4):1147–1155. doi: 10.1093/genetics/142.4.1147. [DOI] [PMC free article] [PubMed] [Google Scholar]

18. Iiri T, Herzmark P, Nakamoto JM, van Dop C, Bourne HR. Rapid GDP release from Gsα in patients with

gain and loss of endocrine function. Nature. 1994;371(6493):164–168. doi: 10.1038/371164a0. [DOI] [PubMed] [Google Scholar]

19. Logan DC. Mitochondrial fusion, division and positioning in plants. Biochem Soc Trans. 2010;38(3):789–795. doi: 10.1042/BST0380789. [DOI] [PubMed] [Google Scholar]

20. Goh LH, et al. Clueless regulates aPKC activity and promotes self-renewal cell fate in Drosophila lgl mutant larval brains. Dev Biol. 2013;381(2):353–364. doi: 10.1016/j.ydbio.2013.06.031. [DOI] [PubMed] [Google Scholar]

21. Gao J, et al. CLUH regulates mitochondrial biogenesis by binding mRNAs of nuclear-encoded mitochondrial proteins. J Cell Biol. 2014;207(2):213–223. doi: 10.1083/jcb.201403129. [DOI] [PMC free article] [PubMed] [Google Scholar]

22. Vinti G, et al. Interactions between hy1 and gun mutants of Arabidopsis, and their implications for plastid/nuclear signalling. Plant J. 2000;24(6):883–894. doi: 10.1046/j.1365-313x.2000.00936.x. [DOI] [PubMed] [Google Scholar]

23. Andersson J, et al. Absence of the Lhcb1 and Lhcb2 proteins of the light-harvesting complex of photosystem II—Effects on photosynthesis, grana stacking and fitness. Plant J. 2003;35(3):350–361. doi: 10.1046/j.1365-313x.2003.01811.x. [DOI] [PubMed] [Google Scholar]

24. Murray DL, Kohorn BD. Chloroplasts of Arabidopsis thaliana homozygous for the ch-1 locus lack chlorophyll b, lack stable LHCPII and have stacked thylakoids. Plant Mol Biol. 1991;16(1):71–79. doi: 10.1007/BF00017918. [DOI] [PubMed] [Google Scholar]

25. Logan DC, Scott I, Tobin AK. The genetic control of plant mitochondrial morphology and dynamics. Plant J. 2003;36(4):500–509. doi: 10.1046/j.1365-313x.2003.01894.x. [DOI] [PubMed] [Google Scholar]

26. Kirchhoff H. Architectural switches in plant thylakoid membranes. Photosynth Res. 2013;116(2-3):481–487. doi: 10.1007/s11120-013-9843-0. [DOI] [PubMed] [Google Scholar]

27. Kong SG, Wada M. Recent advances in understanding the molecular mechanism of chloroplast photorelocation movement. Biochim Biophys Acta. 2014;1837(4):522–530. doi: 10.1016/j.bbabio.2013.12.004. [DOI] [PubMed] [Google Scholar]

28. Chaerle L, Leinonen I, Jones HG, Van Der Straeten D. Monitoring and screening plant populations with combined thermal and chlorophyll fluorescence imaging. J Exp Bot. 2007;58(4):773–784. doi: 10.1093/jxb/erl257. [DOI] [PubMed] [Google Scholar]

29. Larkin RM, Alonso JM, Ecker JR, Chory J. GUN4, a regulator of chlorophyll synthesis and intracellular

signaling. Science. 2003;299(5608):902–906. doi: 10.1126/science.1079978. [DOI] [PubMed] [Google Scholar]

30. Mochizuki N, Brusslan JA, Larkin R, Nagatani A, Chory J. Arabidopsis genomes uncoupled 5 (GUN5) mutant reveals the involvement of Mg-chelatase H subunit in plastid-to-nucleus signal transduction. Proc Natl Acad Sci USA. 2001;98(4):2053–2058. doi: 10.1073/pnas.98.4.2053. [DOI] [PMC free article] [PubMed] [Google Scholar]

31. Adhikari ND, et al. GUN4-porphyrin complexes bind the ChlH/GUN5 subunit of Mg-chelatase and promote chlorophyll biosynthesis in Arabidopsis. Plant Cell. 2011;23(4):1449–1467. doi: 10.1105/tpc.110.082503. [DOI] [PMC free article] [PubMed] [Google Scholar]

32. Karperien A, Ahammer H, Jelinek HF. Quantitating the subtleties of microglial morphology with fractal analysis. Front Cell Neurosci. 2013;7:3. doi: 10.3389/fncel.2013.00003. [DOI] [PMC free article] [PubMed] [Google Scholar]

33. Hanson MR, Sattarzadeh A. Stromules: Recent insights into a long neglected feature of plastid morphology and function. Plant Physiol. 2011;155(4):1486–1492. doi: 10.1104/pp.110.170852. [DOI] [PMC free article] [PubMed] [Google Scholar]

34. Pyke KA, Rutherford SM, Robertson EJ, Leech RM. arc6, a fertile Arabidopsis mutant with only two mesophyll cell chloroplasts. Plant Physiol. 1994;106(3):1169–1177. doi: 10.1104/pp.106.3.1169. [DOI] [PMC free article] [PubMed] [Google Scholar]

35. Chen M, Chory J. Phytochrome signaling mechanisms and the control of plant development. Trends Cell Biol. 2011;21(11):664–671. doi: 10.1016/j.tcb.2011.07.002. [DOI] [PMC free article] [PubMed] [Google Scholar]

36. Osteryoung KW, Stokes KD, Rutherford SM, Percival AL, Lee WY. Chloroplast division in higher plants requires members of two functionally divergent gene families with homology to bacterial ftsZ. Plant Cell. 1998;10(12):1991–2004. doi: 10.1105/tpc.10.12.1991. [DOI] [PMC free article] [PubMed] [Google Scholar]

37. Peragine A, Yoshikawa M, Wu G, Albrecht HL, Poethig RS. SGS3 and SGS2/SDE1/RDR6 are required for juvenile development and the production of trans-acting siRNAs in Arabidopsis. Genes Dev. 2004;18(19):2368–2379. doi: 10.1101/gad.1231804. [DOI] [PMC free article] [PubMed] [Google Scholar]

38. Brandizzi F, Fricker M, Hawes C. A greener world: The revolution in plant bioimaging. Nat Rev Mol Cell Biol. 2002;3(7):520–530. doi: 10.1038/nrm861. [DOI] [PubMed] [Google Scholar]

39. Brandizzi F, et al. ER quality control can lead to retrograde transport from the ER lumen to the cytosol and the nucleoplasm in plants. Plant J. 2003;34(3):269–281. doi: 10.1046/j.1365-313x.2003.01728.x. [DOI] [PubMed] [Google Scholar]

40. Heim DR, Larrinua IM. Primary site of action of amitrole in Arabidopsis thaliana involves inhibition of root elongation but not of histidine or pigment biosynthesis. Plant Physiol. 1989;91(3):1226–1231. doi: 10.1104/pp.91.3.1226. [DOI] [PMC free article] [PubMed] [Google Scholar]

41. Mullineaux PM, Baker NR. Oxidative stress: Antagonistic signaling for acclimation or cell death? Plant Physiol. 2010;154(2):521–525. doi: 10.1104/pp.110.161406. [DOI] [PMC free article] [PubMed] [Google Scholar]

42. Takatsuka H, Umeda M. Hormonal control of cell division and elongation along differentiation trajectories in roots. J Exp Bot. 2014;65(10):2633–2643. doi: 10.1093/jxb/ert485. [DOI] [PubMed] [Google Scholar]

43. Stefano G, Renna L, Moss T, McNew JA, Brandizzi F. In Arabidopsis, the spatial and dynamic organization of the endoplasmic reticulum and Golgi apparatus is influenced by the integrity of the C-terminal domain of RHD3, a non-essential GTPase. Plant J. 2012;69(6):957–966. doi: 10.1111/j.1365-313X.2011.04846.x. [DOI] [PubMed] [Google Scholar]

44. Wang H, Lockwood SK, Hoeltzel MF, Schiefelbein JW. The ROOT HAIR DEFECTIVE3 gene encodes an evolutionarily conserved protein with GTP-binding motifs and is required for regulated cell enlargement in Arabidopsis. Genes Dev. 1997;11(6):799–811. doi: 10.1101/gad.11.6.799. [DOI] [PubMed] [Google Scholar]

45. Jarvis P, López-Juez E. Biogenesis and homeostasis of chloroplasts and other plastids. Nat Rev Mol Cell Biol. 2013;14(12):787–802. doi: 10.1038/nrm3702. [DOI] [PubMed] [Google Scholar]

46. Yang Y, et al. CLUMPED CHLOROPLASTS 1 is required for plastid separation in Arabidopsis. Proc Natl Acad Sci USA. 2011;108(45):18530–18535. doi: 10.1073/pnas.1106706108. [DOI] [PMC free article] [PubMed] [Google Scholar]

47. Chen Y, et al. Plant cells without detectable plastids are generated in the crumpled leaf mutant of Arabidopsis thaliana. Plant Cell Physiol. 2009;50(5):956–969. doi: 10.1093/pcp/pcp047. [DOI] [PubMed] [Google Scholar]

48. Robertson EJ, Pyke KA, Leech RM. arc6, an extreme chloroplast division mutant of Arabidopsis also alters proplastid proliferation and morphology in shoot and root apices. J Cell Sci. 1995;108(Pt 9):2937–2944. doi: 10.1242/jcs.108.9.2937. [DOI] [PubMed] [Google Scholar]

49. Ii JA, Webber AN. Photosynthesis in Arabidopsis thaliana mutants with reduced chloroplast number.

Photosynth Res. 2005;85(3):373–384. doi: 10.1007/s11120-005-7708-x. [DOI] [PubMed] [Google Scholar]

50. Schmitz AJ, Glynn JM, Olson BJ, Stokes KD, Osteryoung KW. Arabidopsis FtsZ2-1 and FtsZ2-2 are functionally redundant, but FtsZ-based plastid division is not essential for chloroplast partitioning or plant growth and development. Mol Plant. 2009;2(6):1211–1222. doi: 10.1093/mp/ssp077. [DOI] [PubMed] [Google Scholar]

51. Raynaud C, et al. Cell and plastid division are coordinated through the prereplication factor AtCDT1. Proc Natl Acad Sci USA. 2005;102(23):8216–8221. doi: 10.1073/pnas.0502564102. [DOI] [PMC free article] [PubMed] [Google Scholar]

52. Jander G, et al. Ethylmethanesulfonate saturation mutagenesis in Arabidopsis to determine frequency of herbicide resistance. Plant Physiol. 2003;131(1):139–146. doi: 10.1104/pp.102.010397. [DOI] [PMC free article] [PubMed] [Google Scholar]

53. Estelle MA, Somerville CR. The mutants of Arabidopsis. Trends Genet. 1986;2:89–93. [Google Scholar]

54. Miyagishima SY, Froehlich JE, Osteryoung KW. PDV1 and PDV2 mediate recruitment of the dynamin-related protein ARC5 to the plastid division site. Plant Cell. 2006;18(10):2517–2530. doi: 10.1105/tpc.106.045484. [DOI] [PMC free article] [PubMed] [Google Scholar]

55. Cookson PJ, et al. Increases in cell elongation, plastid compartment size and phytoene synthase activity underlie the phenotype of the high pigment-1 mutant of tomato. Planta. 2003;217(6):896–903. doi: 10.1007/s00425-003-1065-9. [DOI] [PubMed] [Google Scholar]

56. Liu Y, et al. Manipulation of light signal transduction as a means of modifying fruit nutritional quality in tomato. Proc Natl Acad Sci USA. 2004;101(26):9897–9902. doi: 10.1073/pnas.0400935101. [DOI] [PMC free article] [PubMed] [Google Scholar]

57. Cox RT, Spradling AC. Clueless, a conserved Drosophila gene required for mitochondrial subcellular localization, interacts genetically with parkin. Dis Model Mech. 2009;2(9-10):490–499. doi: 10.1242/dmm.002378. [DOI] [PMC free article] [PubMed] [Google Scholar]

58. Tamura K, Hara-Nishimura I. Functional insights of nucleocytoplasmic transport in plants. Front Plant Sci. 2014;5:118. doi: 10.3389/fpls.2014.00118. [DOI] [PMC free article] [PubMed] [Google Scholar]

59. Asada K. Production and scavenging of reactive oxygen species in chloroplasts and their functions. Plant Physiol. 2006;141(2):391–396. doi: 10.1104/pp.106.082040. [DOI] [PMC free article] [PubMed] [Google Scholar]

Associated Data

This section collects any data citations, data availability statements, or supplementary materials included in this article.

Supplementary Materials

Supplementary File

pnas.1515741113.sapp.pdf (33.7MB, pdf)

Supplementary File

Download video file (704.1KB, avi)

Supplementary File

Download video file (484.4KB, avi)